Electronic Supplementary Material (ESI) for Physical Chemistry Chemical Physics.

Supporting Information

Lateral Diffusion of Ions near Membrane Surface

Subhasish Mallick and Noam Agmon*

The Fritz Haber Research Center, Institute of Chemistry, The Hebrew University of Jerusalem, Jerusalem 9190401, Israel

E-mail: agmon@fh.huji.ac.il

Contents

List of Figures **S3**

S1 Details of the equilibration steps **S9**

S2 Counts.tcl: For counting time average number of atoms in a selected region **S12**

S3 Water_bridge.tcl: Finds probability of Cl^- to bind to the choline methyl groups via water bridges. **S13**

S4 Final_avg_HB_dist.tcl: Calculates the average distance of CH$\cdots$O HBs. **S16**

S5 A Brief Theory of the PME method **S19**

S6 Charge Distribution and ESP for a POPC Membrane Solvated in 400 mM NaCl **S21**

S7 CNN.tcl: Conditional number of neighbors for an atom in a given selection **S23**

S8 Anion hydration **S37**

S9 Diffusion Coefficient Calculations **S43**

References **S51**

List of Figures

S1 The lipid tail C-H order parameter (-S_{CH}) calculated for (a) the palmitoyl (PA) and (b) the oleoyl (OL) chains from our Lipid17 simulation conducted in a 150 mM NaCl solution (depicted in green). It is compared with simulation data using the OPLS-AA FF by Piggot et al.[1] (in blue) and experimental data by Ferreira et al.[2] (in black). S11

S2 (a, b) The time-dependent RMSD calculated for (a) the Oleoyl lipidic chain (in green) and (b) the palmitoyl lipidic chain (in blue) from our 100 ns trajectory, using the VMD RMSD trajectory tools with the initial frame as a reference. (c, d) The total energy and system temperature, respectively, observed over the same 100 ns period for the entire system. S11

S3 Radial pair distribution functions (RDFs) for ions around lipid head groups with (a) the selections "resname PC" and "element K", and (b) the selections "resname PC" and "element Na". Vertical dashed lines mark the location of r_{min}, which is 3.0 Å for K^+ and 2.7 Å for Na^+. These values serve as cutoffs for defining "surface cations" in this work. S19

S4 The ESP for various atom selections, as a function of Z, averaged over the X,Y plane and the 10000 frames of our 100 ns trajectory at a grid size of (a) 1 Å (b) 0.5 Å. The bilayer center is positioned at Z=0 Å. S20

S5 (a) The average charge density derived by taking the second derivative of the analytically fitted polynomial to the ESP data and (b) comparing it with the numerical charge density values for the lipid. S20

S6 The average charge density (a), and the averaged ESP (b) for various atom selections, as a function of Z, averaged over the X,Y plane and the 10000 frames of our 100 ns trajectory (Lipid17 FF, and 400 mM NaCl solution). The obtained values were further smoothed by consecutive four point averaging (two preceding points and two following points). The bilayer center is positioned at Z=0 Å. S21

S7 The distribution of lipid head-group atoms around a surface cation in comparison to the *scaled* distribution of cations around the lipid head-group, for (a) K^+ and (b) Na^+. In both cases the two $g(r)$ distributions coincide for the first peak, nearly coincide at the first minimum, but do not coinside at larger separations. S25

S8 Integration of the radial pair distributions for different types of lipidic oxygen atoms in proximity to a given surface cation: (a) K^+ that is within 3 Å of lipid head groups and (b) Na^+ within 2.7 Å of lipid head groups. Different colors are used to represent different oxygen atoms. The integration values up to their respective first RDF minima are indicated near the corresponding legends. S25

S9 The distances for several K^+ ions from the center of the membrane as a function of time during the 100 ns trajectory. This trajectory has not been unwrapped, so that the ion is reflected back at the periodic boundary $Z = 53.7$ Å. S26

S9 The distances for several K^+ ions from the center of the membrane as a function of time during the 100 ns trajectory. S27

S9 The distances for several K^+ ions from the center of the membrane as a function of time during the 100 ns trajectory. S28

S9 The distances for several K^+ ions from the center of the membrane as a function of time during the 100 ns trajectory. S29

S9 The distances for several K^+ ions from the center of the membrane as a function of time during the 100 ns trajectory. S30

S10 The distances for several Na^+ ions from the center of the membrane as a function of time during the 100 ns trajectory. In comparison with Figure S9, the Na^+ diffusion exhibits longer epochs of binding to the membrane, concomitant with its smaller ionic radius and thus larger affinity to the membranal oxygen atoms as compared with K^+. S31

S10 The distances for several Na^+ ions from the center of the membrane as a function of time during the 100 ns trajectory. S32

S10 The distances for several Na^+ ions from the center of the membrane as a function of time during the 100 ns trajectory. S33

S11 Extracted structures from our MD simulations for interactions of K^+ with the membrane surface with (a) 1 lipid head group through phosphatic oxygen ($O_{PO_4^-}$) (b) 1 lipid head group through carbonyl oxygen O_{CO} (c) 2 lipid head groups through 2 $O_{PO_4^-}$ (d) 2 lipid head groups through 1 $O_{PO_4^-}$ and 1 O_{CO} (e) 2 lipid head groups through 2 O_{CO} (f) 3 lipid head groups through 2 $O_{PO_4^-}$ and 1 O_{CO} (g) 3 lipid head groups through 1 $O_{PO_4^-}$ and 2 O_{CO} (h) 3 lipid head groups through 3 O_{CO}. S34

S12 (a) RDFs and (b) their indefinite integrals for water oxygens (O_w) around K^+ (dark violet line) and Na^+ (dark red line) ions in salty water (400 mM KCl and 400 mM NaCl solutions, without the membrane). In (a) the vertical lines indicate the positions of the first RDF minima. (b) shows the first shell hydration numbers, which are 6.75 for K^+ and 5.87 for Na^+. The dashed lines illustrate how the number of nearest neighbors (contributing to the first hydration shell) were calculated from the first RDF minima. S35

S13 Comparison of hydration structure distribution between "bulk K^+" above membrane system (represented in blue color) and K^+ in pure 400 mM KCl solution (represented in green color). S35

S14 The *scaled* RDF for O_W atoms surrounding (a) bulk K^+ or (b) bulk Na^+ (blue line), superimposed on the RDF for water around a surface cation (red line). Scaling factors of 0.7174 and 0.6297 were applied for K^+ and Na^+, respectively. The first peak for the surface- and bulk-scaled-RDF are nearly identical, reflecting the partial absence of water ligands around a surface-cation. S36

S15 Time evolution of the total (water + lipid) coordination number (CN) is depicted by the upper curve and left Y-axis for (a, b) K^+ (dark-violet line), and (c, d) Na^+ (dark-red line). The number of interacting lipid head groups is shown by the lower blue curve and the right Y-axis. This shows that the total CN is almost constant, irrespective of the number of water ligands that gets replaced by lipid atoms. The indexes of the selected K^+ and Na^+ ions correspond to those in Figure 10 of the main text. S36

S16 Radial pair distribution functions (a) and their indefinite integrals (b) for water oxygen atoms (O_w) around a Cl^- ion in the bulk (blue line) and within 2.9 Å from the membrane surface (red line) or, specifically, from the choline group (both conditions generate the same RDF). The inset represents the zoomed plot for the first hydration shell with dashed lines showing how the number of nearest neighbors is calculated. S37

S17 Distances of two representative Cl^- ions from the center of the membrane (green line and left Y-axis) along with the number of interacting lipid head groups (orchid line and right Y-axis) as a function of time during the 100 ns trajectory. The dotted line represents the average position of the membrane surface at $\sim$ 20 Å. In our distance calculations the trajectory has not been unwrapped. S38

S18 The distances for several Cl^- ions from the center of the membrane as a function of time during the 100 ns (wrapped, Gromacs) trajectory. S39
S18 The distances for several Cl^- ions from the center of the membrane as a function of time during the 100 ns (wrapped, Gromacs) trajectory. S40
S18 The distances for several Cl^- ions from the center of the membrane as a function of time during the 100 ns (wrapped, Gromacs) trajectory. S41
S18 The distances for several Cl^- ions from the center of the membrane as a function of time during the 100 ns (wrapped, Gromacs) trajectory. S42
S19 Mean square displacement (MSD) plots (up to 50 ns) for the phosphorus atoms of the POPC head groups solvated in (a) 0 mM salt, (b) 150 mM NaCl, (c) 150 mM KCl, (d) 400 mM KCl, and (e) 400 mM NaCl solutions, using the Lipid17 FF. Green dotted lines represent linear fits in the range 10 to 50 ns, from which D_L was extracted (Table 7a). S45
S20 MSD plots (up to 50 ns) for the phosphorus atoms of the POPC head groups solvated in (a) 0 mM salt, (b) 150 mM NaCl, and (c) 400 mM NaCl solution using the Lipid21 FF. Green dotted lines represent the linear fitted lines within 10 to 50 ns, from which D_L was extracted (Table 7b). S45
S21 MSD plots for (a) the phosphorus atom of the POPC head group solvated in 150 mM KCl (red line), 150 mM NaCl (green line), and 400 mM KCl (blue line); (b) Lipid self-diffusion in 150 mM KCl (red), compared to surface K^+ in 150 mM KCl solution (violet), and surface Na^+ in 150 mM NaCl solution (brown), using the Lipid17 FF. S46
S22 MSD plot illustrating lipid self-diffusion (blue) and surface Na^+ diffusion (brown) in (a) 400 mM NaCl solution, and (b) 150 mM NaCl solution using the Lipid21 force field. Evidently, the cation lateral diffusion is notably faster than lipid self-diffusion. S46

S23 The MSD in the X,Y plane as a function of time (0–10 ns) for: (a) bulk K^+ in 400 mM KCl, (b) bulk K^+ in 150 mM KCl, (c) K^+ in 400 mM aqueous KCl solution, (d) bulk Na^+ in 400 mM NaCl, (e) bulk Na^+ in 150 mM NaCl, and (f) Na^+ in 400 mM aqueous NaCl solution. The dotted lines represent power-law fits. The power, α, is close to 1, indicative of normal cation diffusion in the bulk (as opposed to the abnormal lateral surface diffusion). S47

S24 Fits of the tine-dependent cationic MSD (0–5 ns) to the double-Flory model, Eq. (3) in main text, for surface ions: (a) K^+ in 150 mM KCl, Lipid17 FF (b) Na^+ in 150 mM NaCl, Lipid17 FF, (c) Na^+ in 400 mM NaCl, Lipid17 FF, (d) Na^+ in 150 mM NaCl, Lipid21 FF, (e) Na^+ in 400 mM NaCl, Lipid21 FF. See also Figure 17 in main text. S47

S25 The top two rows illustrate the temporal evolution of the Cartesian coordinates (only X and Y) for representative Na^+ (index 10733, left column) and K^+ (index 10747, right column) ions. Lower panels display the distances between these cations and their neighbouring Pi atoms of lipid head groups within the same designated time interval. S48

S26 Temporal evolution of the distances between some representative Na^+ ions and their neighbouring Pi atoms of lipid head groups during various time spans. S49

S27 Temporal evolution of the distances between some representative K^+ ions and their neighbouring Pi atoms of lipid head groups during various time spans. S50

S1 Details of the equilibration steps

The system has been equilibrated for a total of 20 ns in six consecutive steps. In each step, we gradually reduced the positional and dihedral restraining force constants (FC), in units of kJ $mol^{-1}nm^{-2}$ and kJ $mol^{-1}rad^{-2}$, respectively. The details are given below:

Step 1:

Simulation time: 125 ps

Time step: 1 fs

Positional restraint of lipid: Force constant (FC) = 1000.0

Dihedral restraint: FC = 1000.0

Step 2:

Simulation time: 125 ps

Time step: 1 fs

Positional restraint of lipid: FC = 400.0

Dihedral restrain: FC = 400.0

Step 3:

Simulation time: 500 ps

Time step: 1 fs

Positional restraint of lipid: FC = 400.0

Dihedral restraint: FC = 200.0

Step 4:

Simulation time: 500 ps

Time step: 2 fs

Positional restraint of lipid: FC = 200.0

Dihedral restrain: FC = 200.0

Step 5:

Simulation time: 500 ps

Time step: 2 fs

Positional restraint of lipid: FC = 40.0

Dihedral restrain: FC = 100.0

Step 6:

Simulation Time: 18 ns

Time step: 2 fs

Position restraint of Lipid: None

Dihedral restrain: None

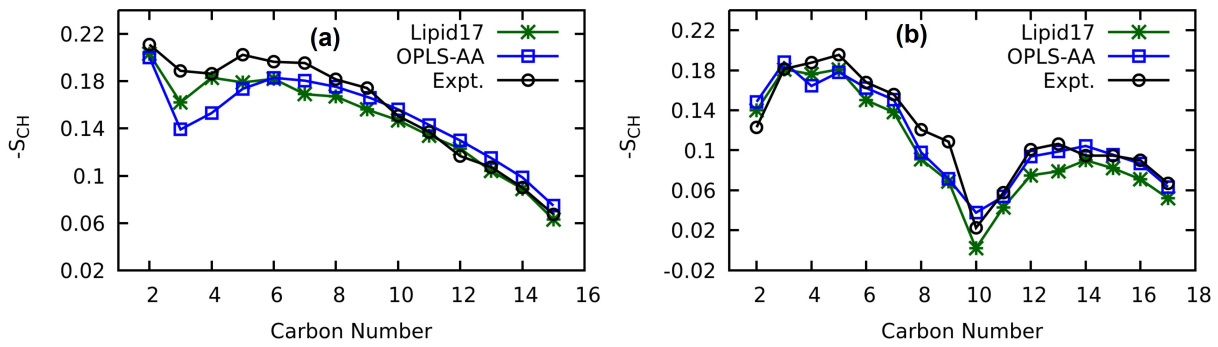

Figure S1: The lipid tail C-H order parameter ($-S_{CH}$) calculated for (a) the palmitoyl (PA) and (b) the oleoyl (OL) chains from our Lipid17 simulation conducted in a 150 mM NaCl solution (depicted in green). It is compared with simulation data using the OPLS-AA FF by Piggot et al.[1] (in blue) and experimental data by Ferreira et al.[2] (in black).

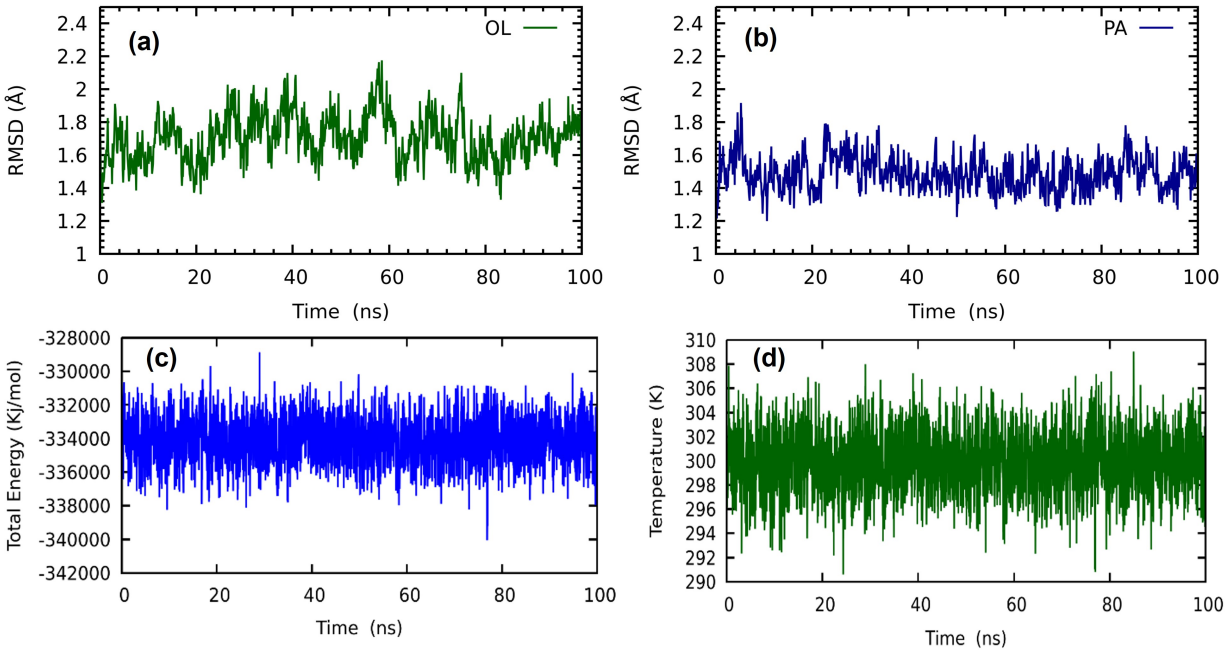

Figure S2: (a, b) The time-dependent RMSD calculated for (a) the Oleoyl lipidic chain (in green) and (b) the palmitoyl lipidic chain (in blue) from our 100 ns trajectory, using the VMD RMSD trajectory tools with the initial frame as a reference. (c, d) The total energy and system temperature, respectively, observed over the same 100 ns period for the entire system.

S2 Counts.tcl: For counting time average number of atoms in a selected region

```
##Usage: number "selection of atoms around selected condition" output.csv #
#############################################################################
proc number {sel_atoms output} {
     # Get the total number of frames in the trajectory
     set nf [molinfo top get numframes]
     # Open output file for writing
     set outfile [open $output w]
     # Write header to output file
     puts $outfile "Frame, Number of atoms, Total atoms, Time-average number of atoms"
     # Initialize variables
     set T_atoms 0.00
     # Loop over each frame
     for {set i 0} {$i < $nf} {incr i} {
       # Select atoms in current frame
       set atoms [atomselect top "$sel_atoms" frame $i]
       $atoms update
       # Get the number of atoms
       set list_atoms [$atoms num]
       # Summation over all the frames
       set T_atoms [expr {$T_atoms + $list_atoms }]
     puts "frame $i of $nf"
     # Write data to output file for this frame
     puts $outfile "$i, $list_atoms,$T_atoms"
       }
       # Estimating time-average number of atoms
     set Avg_atom [expr {$T_atoms / $nf}]
```

```
     puts "Time-average number of atoms = $Avg_atom"
     puts $outfile ", , ,$Avg_atom"
       close $outfile
}
##########################################################################
```

S3 Water_bridge.tcl: Finds probability of Cl^- to bind to the choline methyl groups via water bridges.

```
# Usage "mass 35.452999" output.file
##############################################
proc bridge {sel1 output} {
    set nf [molinfo top get numframes]
    set outfile [open $output w]
#Cut-off value for the distance of Cl from membrane center
    set Z_max 29.0
# Center of max in Z direction
set Z_COM 57.825
    #Cut-off value for Cl solvation by cholinic methyl, C_Me
    set cutoff 5.
set n_Cl_tot 0
set n_Cl_bound_tot 0
set n_C_Me_tot 0
set n_surf 0
#loop over frames
puts "loop over frames"
    for {set i 0} {$i < $nf} {incr i} {
puts "Frame $i"
```

```
puts $outfile "Frame $i"
        set sel [atomselect top "$sel1" frame $i]
set Cl_list {}
set O_list {}
# z value and index from the same input selection
set ZZ [$sel get z]
set Cl [$sel get index]
set n_Cl [$sel num]
set n_Cl_tot [expr {$n_Cl_tot + $n_Cl}]
set n_surf1 0
set j 0
set n_Cl_bound 0

        #Loop over selected Cl atoms
        foreach Z $ZZ {
#resetting Z-origin at center of membrane
set Z1 [expr {abs ($Z - $Z_COM)} ]
if {$Z1 < $Z_max} {
# The trick: skip indices that do not obey the condition on Z
set Cl_j [lindex $Cl $j]
lappend Cl_list $Cl_j
incr n_surf1
# find cholinic methyl carbons within HB distance of chosen Cl ...
set selC_Me [atomselect top "name C33 C34 C35 and within
 $cutoff of index $Cl_j" frame $i]
set C_Me [$selC_Me get index]
# ... and count them
set n_C_Me [$selC_Me num]
# if at least one Me, consider as bound Cl
```

```
if {$C_Me != ""} {
incr n_Cl_bound
### Find water oxygens in contact with both Cl and a methyl carbon
foreach C $C_Me {
set selO [atomselect top "name O and (within 3.7 of index $Cl_j)
 and (within 3.5 of index $C)" frame $i]
set OW [$selO get index]
lappend O_list $OW
}
puts  "$j index Cl $Cl_j   number C_Me $n_C_Me index
 C_Me $C_Me   index OW  $OW"
puts $outfile "$j index Cl $Cl_j   number C_Me $n_C_Me
index C_Me $C_Me   index OW  $OW"
}
#puts  "index Cl $Cl_j   number C_Me $n_C_Me index C_Me $C_Me
  OW  $OW"
}
# index of the Cl atom list
incr j
}
# Counts for each frame
set n_surf [expr {$n_surf + $n_surf1}]
puts "number Cl on surface: $n_surf1 , of which bound: $n_Cl_bound"
puts $outfile "number Cl on surface: $n_surf1 , of which bound: $n_Cl_bound"
set n_Cl_bound_tot [expr {$n_Cl_bound_tot + $n_Cl_bound} ]
}
# Averaging over all frames
set f_surf [expr {($n_surf + 0.0) / $n_Cl_tot}]
puts " "
```

```
puts "Total over all frames:"
puts "fraction of Cl on surface (up to $Z_max A from center): $f_surf"
puts $outfile  "Total over all frames:"
puts $outfile  "fraction of Cl on surface (up to $Z_max A from center): $f_surf"
set f_bound [expr { ( $n_Cl_bound_tot + 0.0 ) / $n_surf } ]
puts "fraction of which is bound to any C_Me: $f_bound"
puts $outfile "fraction of which is bound to any C_Me: $f_bound"

close $outfile
}

##########################################################################
```

S4 Final_avg_HB_dist.tcl: Calculates the average distance of CH$\cdots$O HBs.

```
# Usage "mass 35.452999" output.file
################################################
proc HB_dist {sel1 output} {
    set nf [molinfo top get numframes]
    set outfile [open $output w]
    #Cut-off value for the first hydration shell of Cl
    set cutoff 4.0
    #Starting of variables
    set total_HB_dist 0.0
    set number_of_HB 0
    #loop over frames
    for {set i 0} {$i < $nf} {incr i} {
```

```
    set Cl_list [atomselect top "$sel1" frame $i]
    set Cl_indexes [$Cl_list get index]
    #Loop over selected Cl atoms
    foreach Cl $Cl_indexes {
#Finds oxygen atoms within the specified cutoff distance from the Cl atom
        set oxygen_atoms [atomselect top "name O and within
        $cutoff of index $Cl" frame $i]
        set O_indexes [$oxygen_atoms get index]
        #loop over oxygen atoms
        foreach oxygen $O_indexes {
            set oxy [atomselect top "index $oxygen" frame $i]
            set Ox [$oxy get x]
            set Oy [$oxy get y]
            set Oz [$oxy get z]
            #Retrieves nearby methylic hydrogen atoms of choline within 3
            units of the oxygen atom.
            set HCs [atomselect top "type H3A H3B H3C H4A H4B H4C H5A H5B H5C
             and within 3 of index $oxygen" frame $i]
            set Hnum [$HCs num]

            if {$Hnum > 0} {
                set Hx [$HCs get x]
                set Hy [$HCs get y]
                set Hz [$HCs get z]
                set number_of_HB [expr {$number_of_HB + $Hnum}]
                #Calculates distances between the oxygen and hydrogen atoms
                foreach hx $Hx hy $Hy hz $Hz {
                    set mind [expr {sqrt(($Ox - $hx) ** 2 + ($Oy - $hy) ** 2
                    + ($Oz - $hz) ** 2)}]
```

```
                        puts $outfile "$i, $oxygen, $mind" ;
                        # Write the distance to the output file

                        # Accumulate the distances within the loop
                        set total_HB_dist [expr {$total_HB_dist + $mind}]
                    }
                } else {
                    puts $outfile "No H-Bond" ;# Write 0 when no hydrogen atoms are found
                }
            }
        }
    }

    # Calculate average distance outside the loop
    set avg_dist 0.0
    if {$number_of_HB > 0} {
        set avg_dist [expr {$total_HB_dist / $number_of_HB}]
    }
    puts "avg dist $avg_dist"
    close $outfile
}

##############################################################################
```

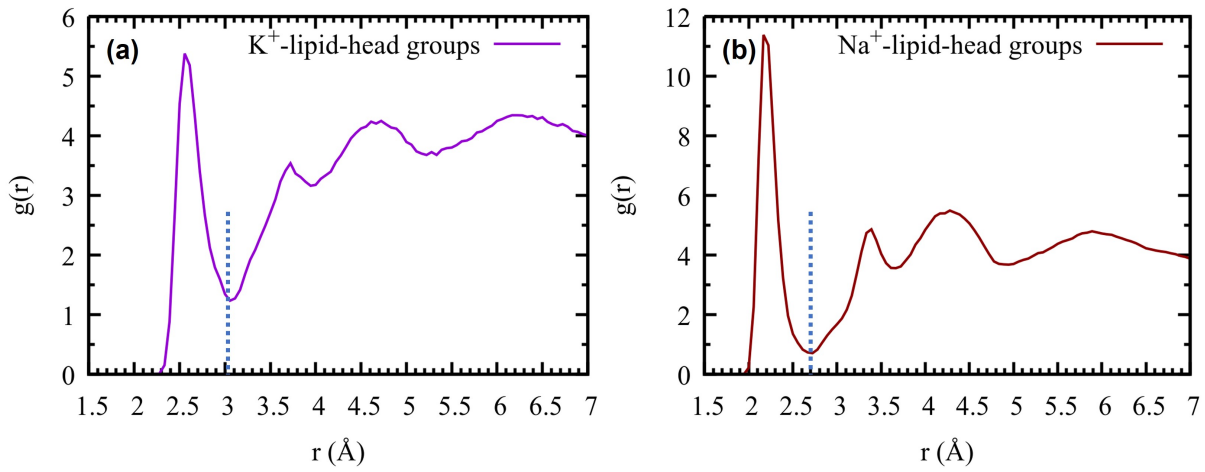

Figure S3: Radial pair distribution functions (RDFs) for ions around lipid head groups with (a) the selections "resname PC" and "element K", and (b) the selections "resname PC" and "element Na". Vertical dashed lines mark the location of r_{min}, which is 3.0 Å for K^+ and 2.7 Å for Na^+. These values serve as cutoffs for defining "surface cations" in this work.

S5 A Brief Theory of the PME method

We have calculated the ESP using the Particle Mesh Ewald (PME) method.[3] It decomposes the Coulomb interaction into two terms: a short-ranged term (fast decaying and computed in real space), and a long-ranged term (slow decaying computed in reciprocal space). The point charges are approximated by spherical Gaussian distributions in three dimensions, normalized to give the charge (q_i) after integration:

$$\rho_i(r) = q_i \left(\frac{\beta}{\sqrt{\pi}}\right)^3 e^{-\beta^2 |r - r_i|^2} \tag{1}$$

where β, a positive parameter, defines the width of the distribution. The electrostatic potential is computed using the Poisson equation:

$$-\nabla^2 \phi(r) = 4\pi \sum_i \rho_i(r) \tag{2}$$

where the sum runs over all atoms. The fast Fourier transformation (FFT) method was used to solve the equation numerically, the accuracy of the solution depending on the grid density.

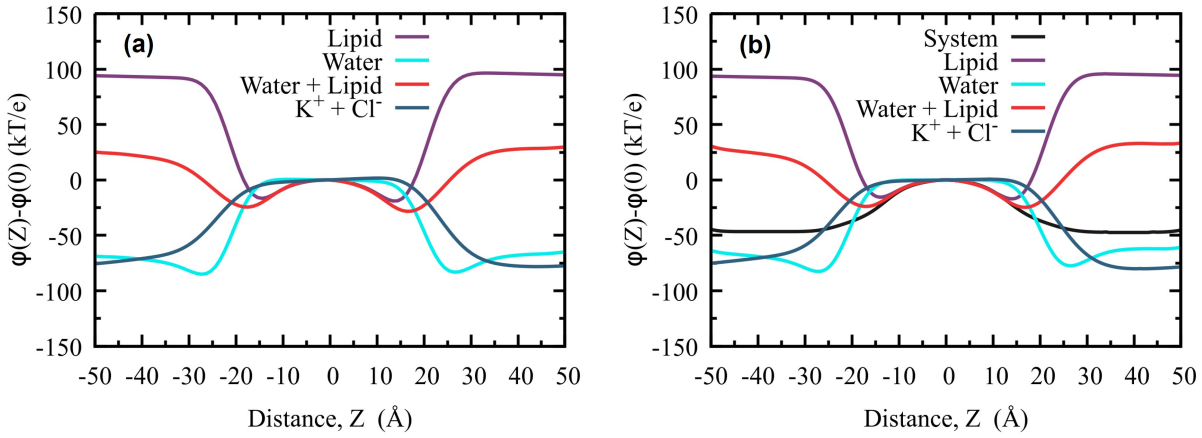

Figure S4: The ESP for various atom selections, as a function of Z, averaged over the X,Y plane and the 10000 frames of our 100 ns trajectory at a grid size of (a) 1 Å (b) 0.5 Å. The bilayer center is positioned at Z=0 Å.

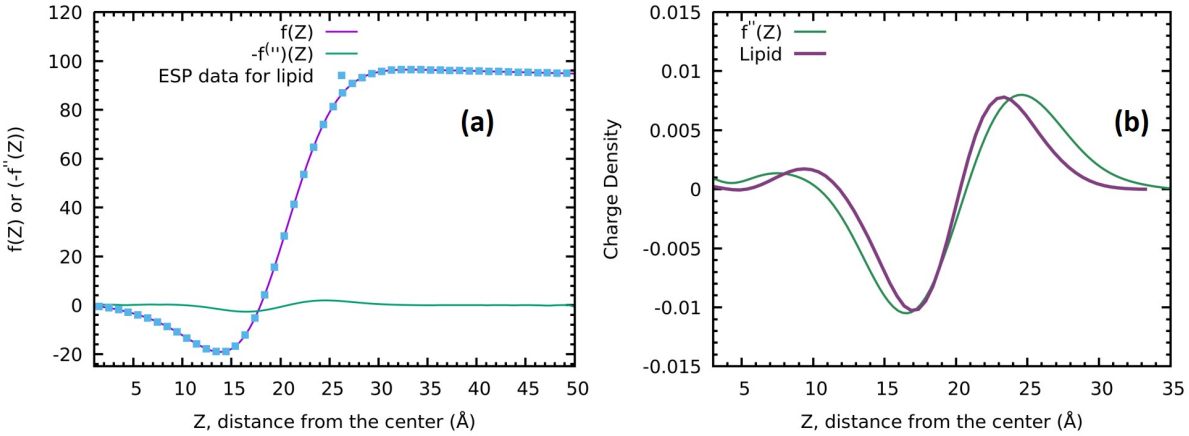

Figure S5: (a) The average charge density derived by taking the second derivative of the analytically fitted polynomial to the ESP data and (b) comparing it with the numerical charge density values for the lipid.

S6 Charge Distribution and ESP for a POPC Membrane Solvated in 400 mM NaCl

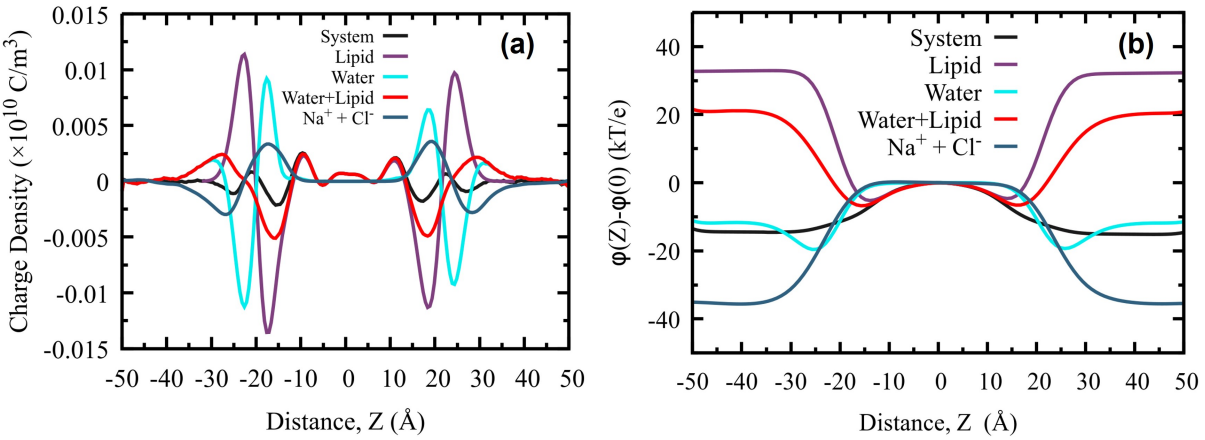

Figure S6: The average charge density (a), and the averaged ESP (b) for various atom selections, as a function of Z, averaged over the X,Y plane and the 10000 frames of our 100 ns trajectory (Lipid17 FF, and 400 mM NaCl solution). The obtained values were further smoothed by consecutive four point averaging (two preceding points and two following points). The bilayer center is positioned at Z=0 Å.

Figure S6a shows the charge distribution for various atom selections for a POPC membrane solvated in 400 mM NaCl solution. This complements the case of KCl in Figure 5 of the main text. While the various charge densities are similar for KCl and NaCl, some quantitative differences can be found. We focus here on the ionic charge densities of Na^+ plus Cl^- (dark blue line), to be compared with K^+ plus Cl^- in Figure 5c of the main text. In each membrane leaflet we find exactly one positive peak (assigned to Na^+) and one negative one (assigned to Cl^-). The locations of these peaks are listed in Table S1.

Table S1: Peak locations (Z, in Å) for the ionic charge densities in the two membrane leaflets, as depicted in Figures 5c and S6a.

	Left leaflet		Right leaflet	
	Cl^-	cation	cation	Cl^-
NaCl	-27.2	-17.6	19.5	28.3
KCl	-28.6	-19.7	17.5	28.6

Comparison between the peaks in the two leaflets, obtained in the same trajectory and

hence expected to be mirror images, teaches us on the error bounds of the calculation. The error for the cations is quite large, their peaks being either 17.5 or 19.5 Å. This is probably due to the noise in the charge density data and its smoothing procedure. The average is thus 18.5 Å, and it is identical for Na^+ and K^+. This contrasts with Vácha et al.[4], who have found specific ion effects on the position of the peak (using mass density rather than charge density, and different lipid and FF). In the present work we have found several differences between these cations, but the peak position is not one of them.

There seems to be less error in the Cl^- peak position, which is nearly identical in the two leaflets, particularly for KCl. This highlights another difference with the literature (e.g., Vácha et al.[4]), which discusses formation of a charged double layer at the membrane surface with positive charges inside and negative charges outside. Once cations bind to the membrane, anions distribute in solution to compensate for the positive layer at the membrane. Such a model is applied in electrochemistry to describe the electrical double layer in the solution adjacent to a charged electrode, which can be approximately described by the Gouy-Chapman (GC) model.[5] To what extent does it describe the ion density near the POPC membrane?

In the GC model, the membrane is a negatively charged plane (due to the phosphatic headgroups), in equilibrium with an electrolyte solution (say, of NaCl). The solution of the GC equations for the mobile ion concentration is monotonically decreasing for unlike charges (Na^+), and monotonically increasing for like charges (Cl^-), see Fig. 3 in Oldham[6] (dashed lines). This is not the case for the ion densities near a membrane (Figure 2b). For example, the Cl^- density increases from 0 at the membrane surface ($Z = 19$ Å) up to a maximum, then decreases to the asymptotic bulk value. This may be interpreted as a superposition of a Gaussian-shaped peak (specific interactions) and the GC solution (continuum electrostatics). The first is due to choline-bound Cl^-, and the latter to all the other mobile chloride ions.

S7 CNN.tcl: Conditional number of neighbors for an atom in a given selection

```
#Usage: CNN "atom selection" output.out
#For e.g., CNN "element K" NN_K.out, which will count average number of neighbouring
#lipid head groups near a K+ ion.
# For each atom in a selection, and each time frame,
# if number of neighbors (NN) > 0 (= the condition)
# add NN to previous and increase number of bound frames
# (when the condition is obeyed)
################################################################################
proc CNN {select output} {
         set outfile [open $output w]
         set sel [atomselect top $select frame 0]
         set selist [$sel list]
    set atomnumber [$sel num]
        #input: minimum in g(r)
        set r_min 2.7
     set nf [molinfo top get numframes]
          puts $outfile "We have a selection of $atomnumber atoms and $nf frames"
          puts stdout "We have a selection of $atomnumber atoms and $nf frames"
         set neighbor 0
#number of frames atom is bound
    set nf_bound 0

        puts $outfile "atomindex frame neighbor nf_bound"
# loop over atomindices
          foreach atomindex $selist {
# loop over frames
```

```
   for {set i 0} {$i < $nf} {incr i} {
     set s2 [atomselect top "resname PC and within $r_min of index $atomindex" frame $i]
# running number of neighbors in each frame
         set newneighbor [$s2 num]
# This can be either >0 or =0, calc is done only in the 1st case
    if {$newneighbor > 0} {
    set nf_bound [expr {$nf_bound + 1}]
    set neighbor [expr {$newneighbor + $neighbor}]
    }
    puts $outfile "$atomindex $i $neighbor $nf_bound"
   }
   }
# end of two loops
   if {$neighbor > 0} {
   set neighbor [expr {($neighbor + 0.0) / $nf_bound}]
   }
# else the routine returns 0
                 puts stdout "number of frames bound $nf_bound"
        puts stdout "Average number of neighbors $neighbor"
      puts $outfile "average number of neighbors $neighbor"
          puts $outfile "number of frames bound $nf_bound"
   close $outfile
}
################################################################################
```

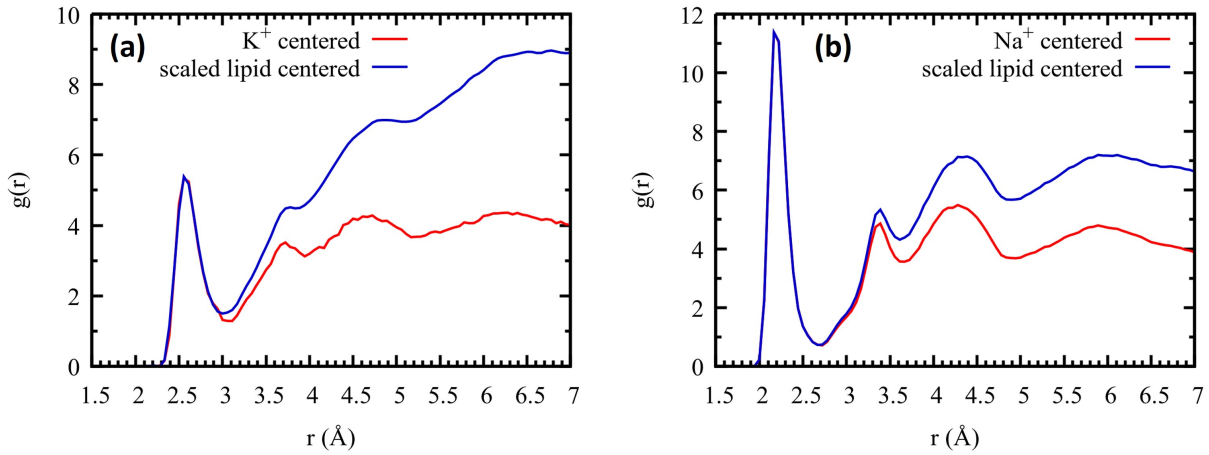

Figure S7: The distribution of lipid head-group atoms around a surface cation in comparison to the *scaled* distribution of cations around the lipid head-group, for (a) K^+ and (b) Na^+. In both cases the two $g(r)$ distributions coincide for the first peak, nearly coincide at the first minimum, but do not coinside at larger separations.

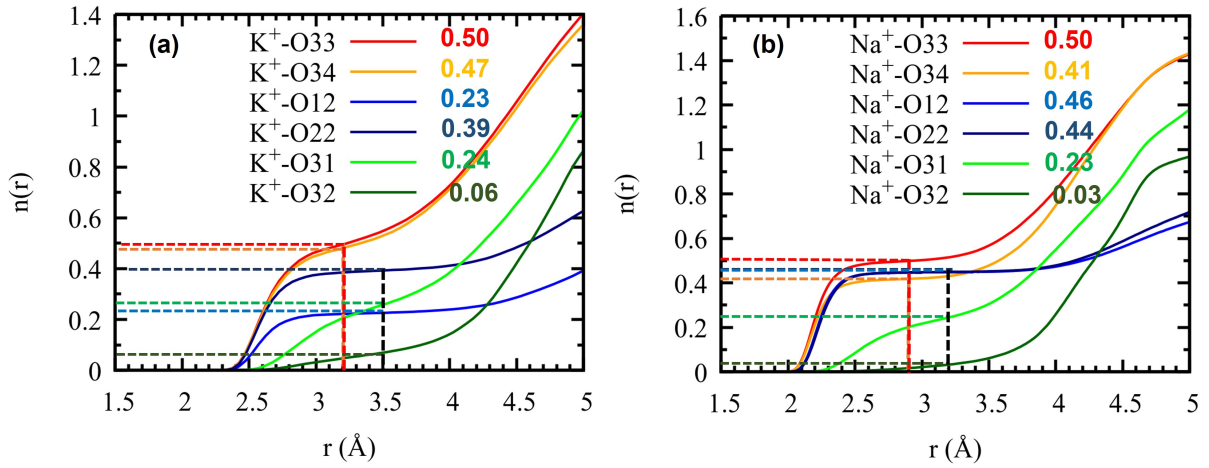

Figure S8: Integration of the radial pair distributions for different types of lipidic oxygen atoms in proximity to a given surface cation: (a) K^+ that is within 3 Å of lipid head groups and (b) Na^+ within 2.7 Å of lipid head groups. Different colors are used to represent different oxygen atoms. The integration values up to their respective first RDF minima are indicated near the corresponding legends.

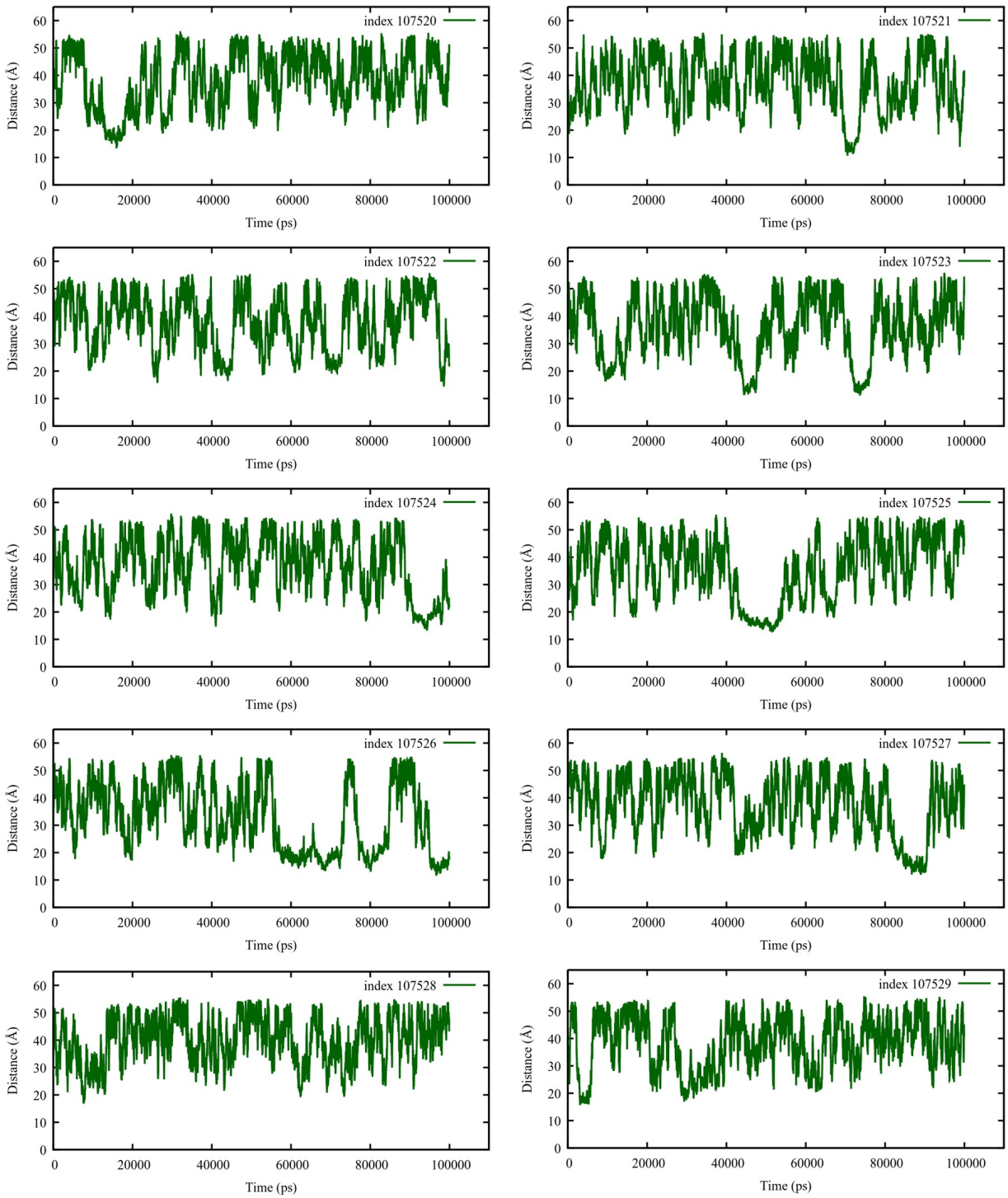

Figure S9: The distances for several K^+ ions from the center of the membrane as a function of time during the 100 ns trajectory. This trajectory has not been unwrapped, so that the ion is reflected back at the periodic boundary $Z = 53.7$ Å.

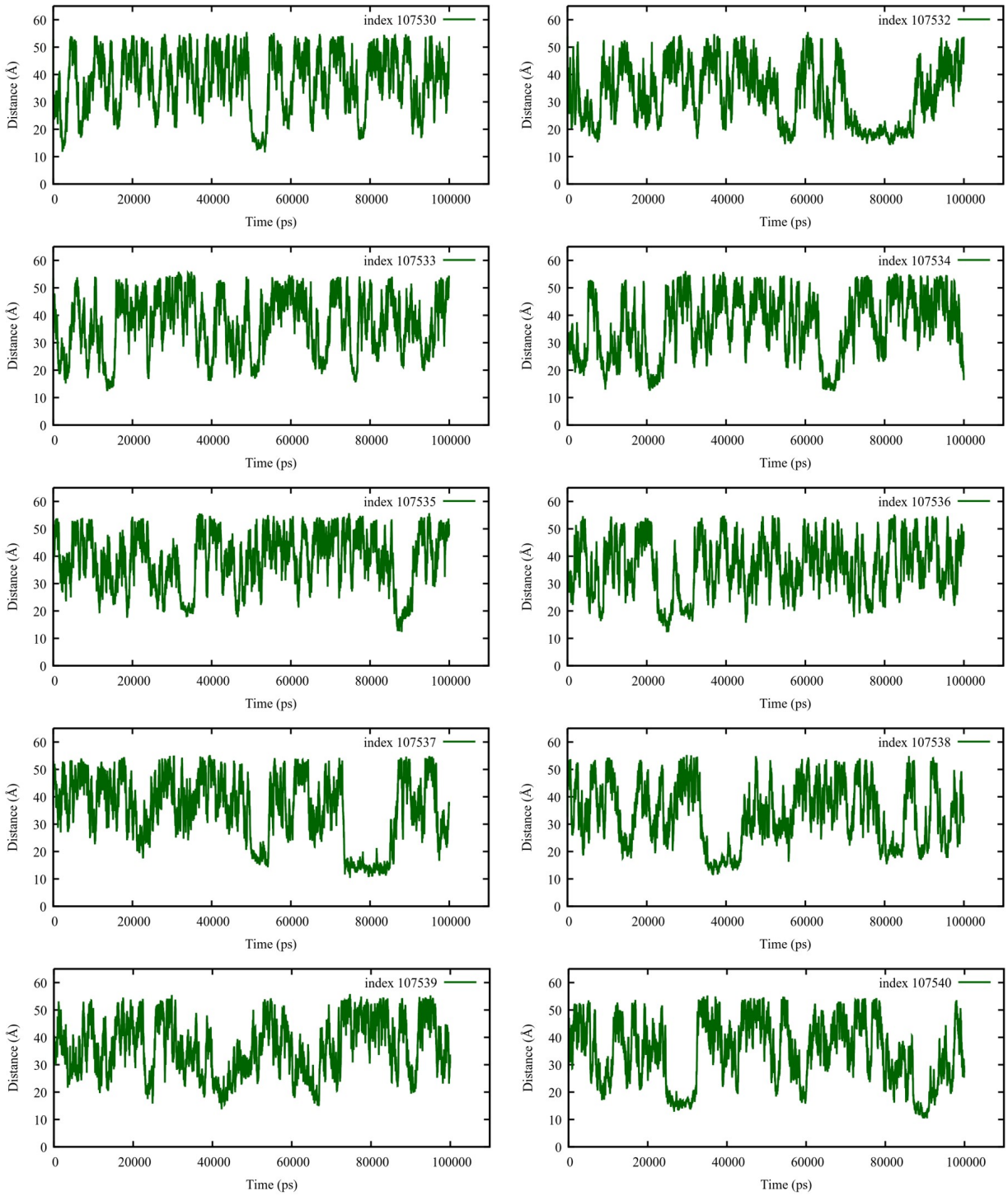

Figure S9: The distances for several K^+ ions from the center of the membrane as a function of time during the 100 ns trajectory.

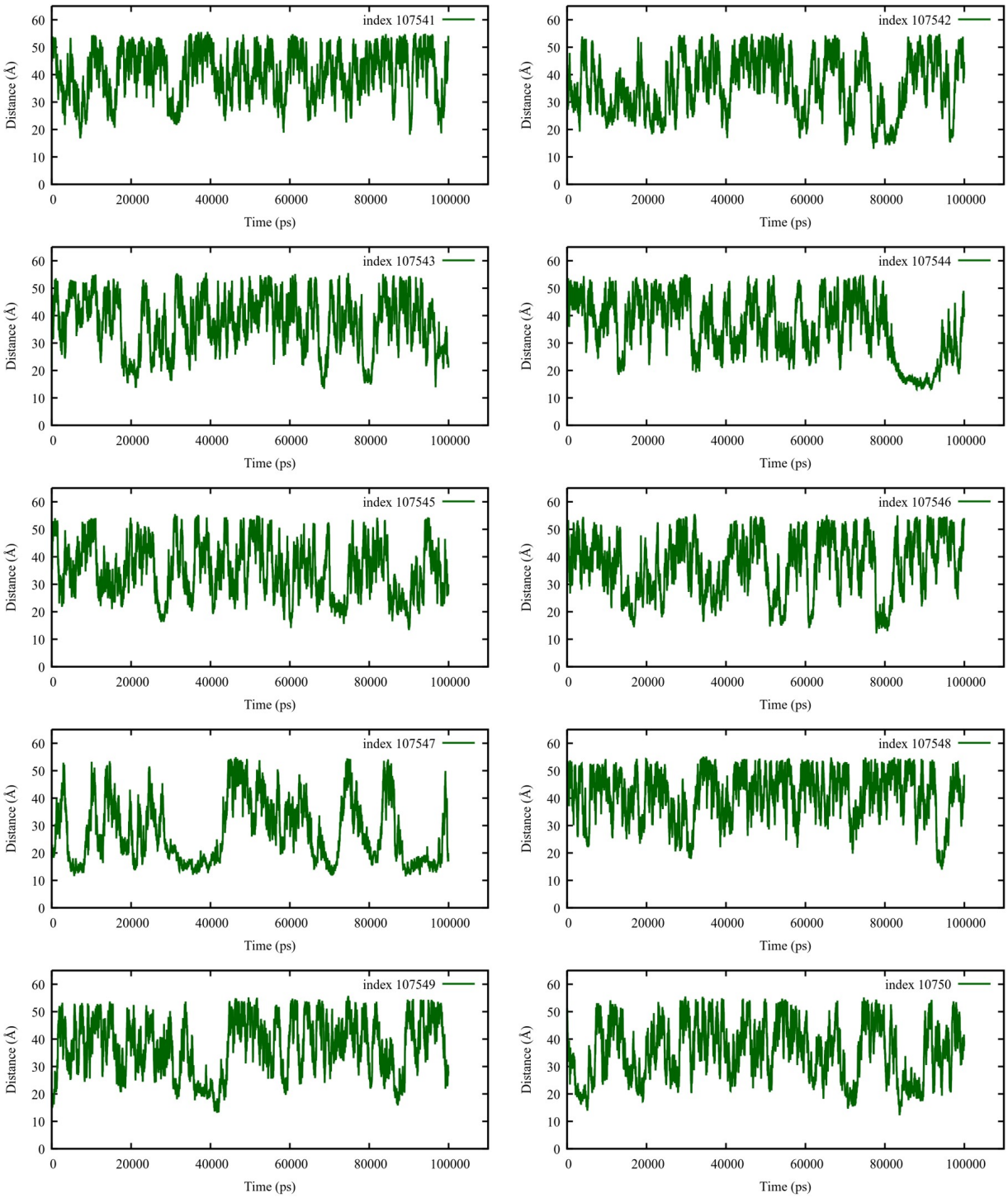

Figure S9: The distances for several K^+ ions from the center of the membrane as a function of time during the 100 ns trajectory.

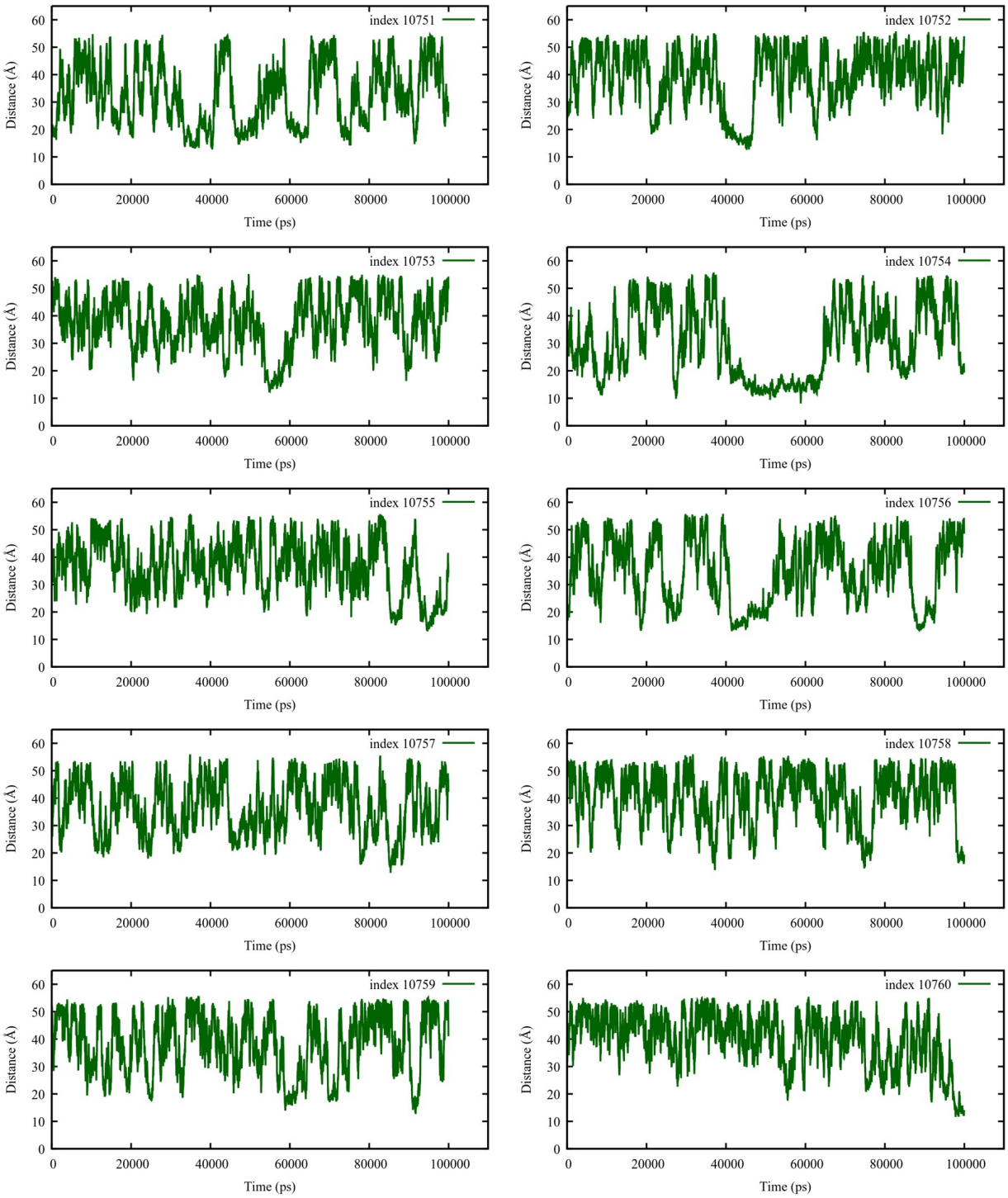

Figure S9: The distances for several K^+ ions from the center of the membrane as a function of time during the 100 ns trajectory.

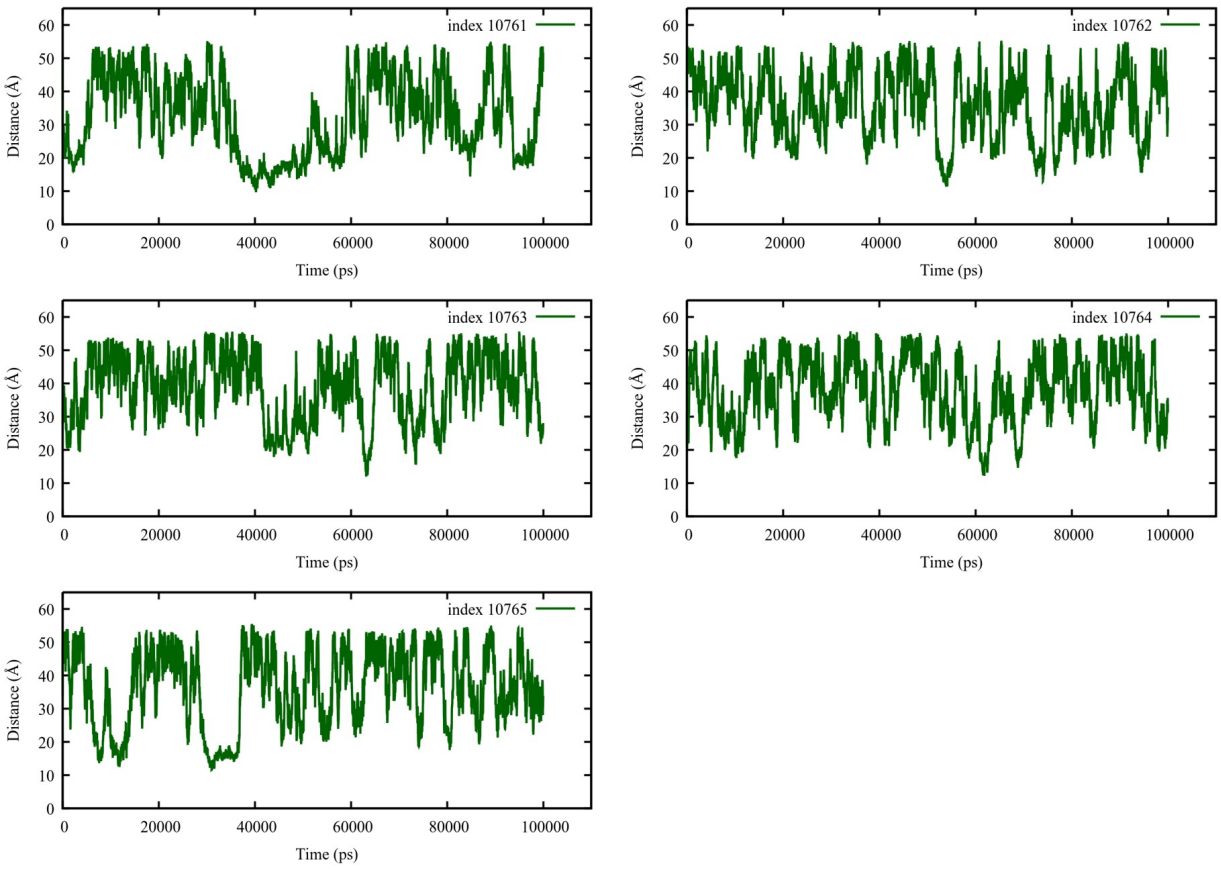

Figure S9: The distances for several K^+ ions from the center of the membrane as a function of time during the 100 ns trajectory.

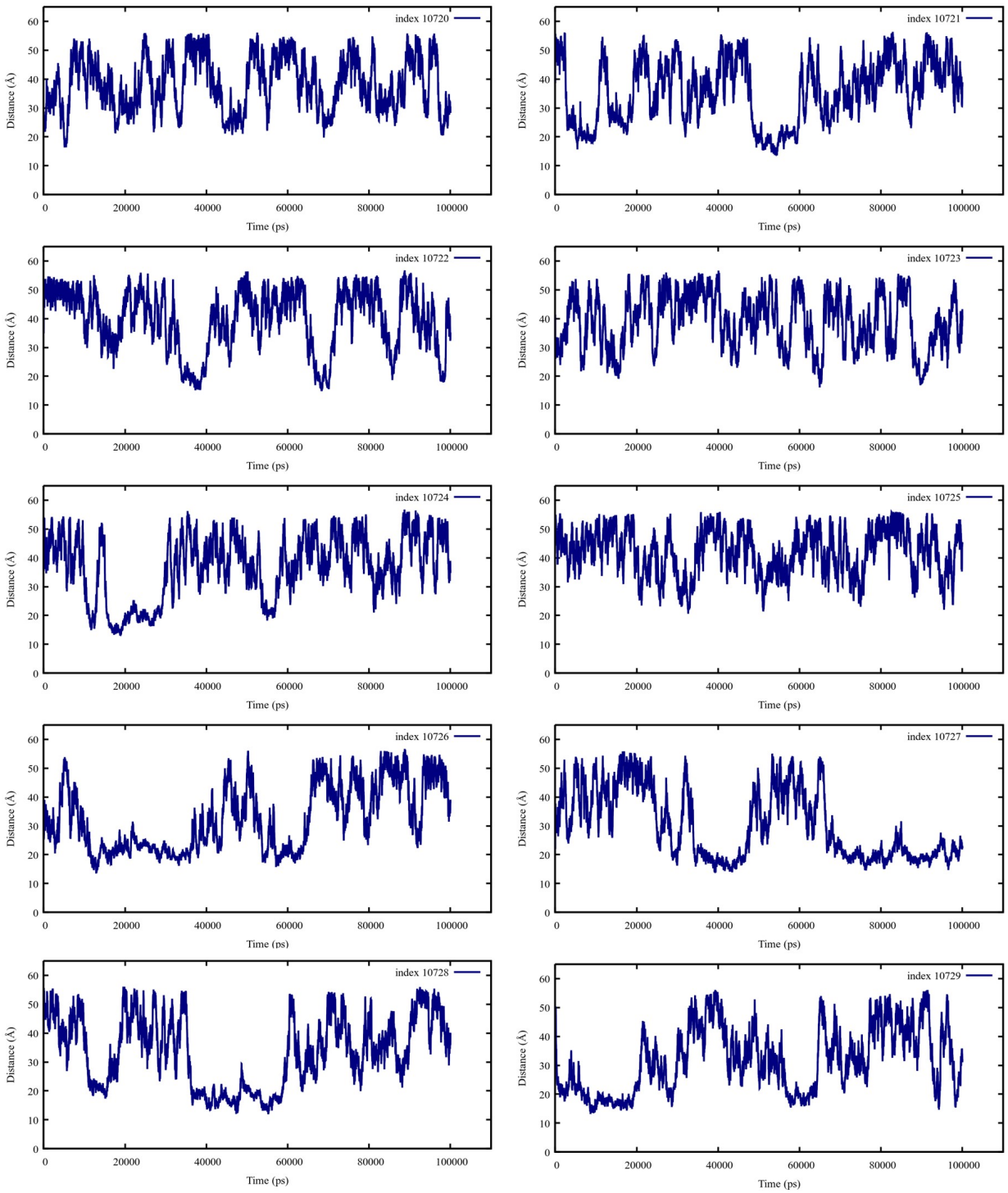

Figure S10: The distances for several Na^+ ions from the center of the membrane as a function of time during the 100 ns trajectory. In comparison with Figure S9, the Na^+ diffusion exhibits longer epochs of binding to the membrane, concomitant with its smaller ionic radius and thus larger affinity to the membranal oxygen atoms as compared with K^+.

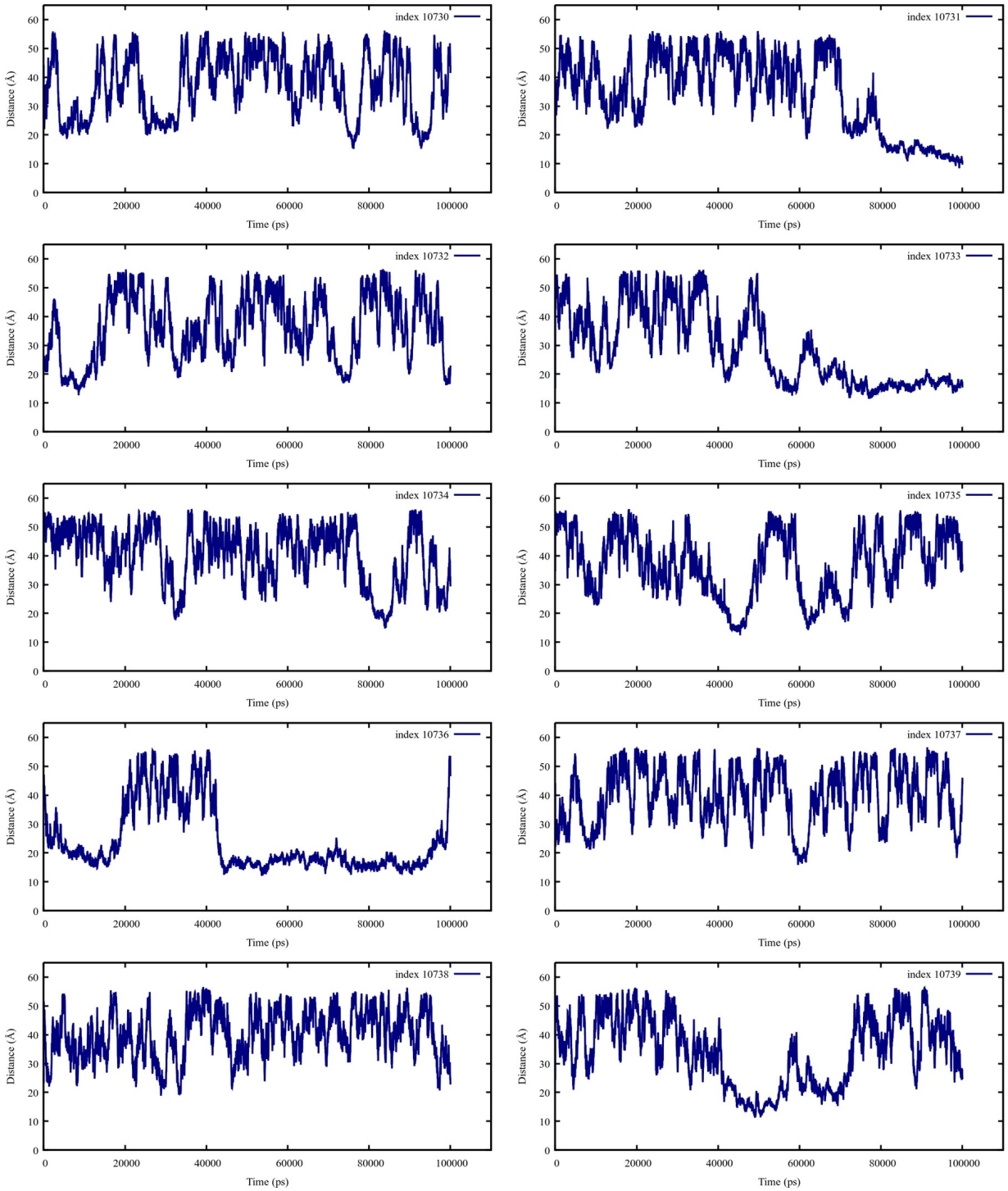

Figure S10: The distances for several Na^+ ions from the center of the membrane as a function of time during the 100 ns trajectory.

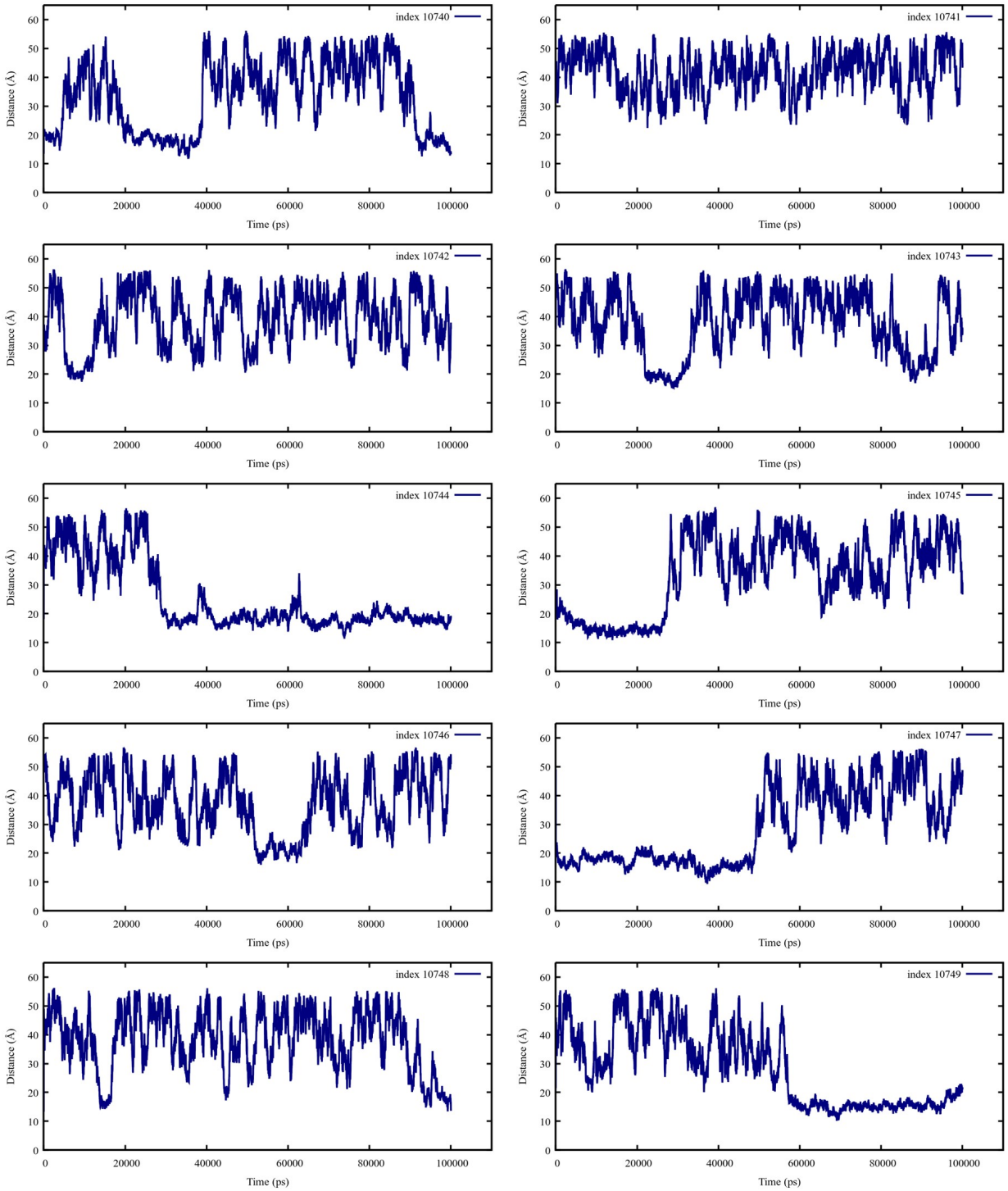

Figure S10: The distances for several Na^+ ions from the center of the membrane as a function of time during the 100 ns trajectory.

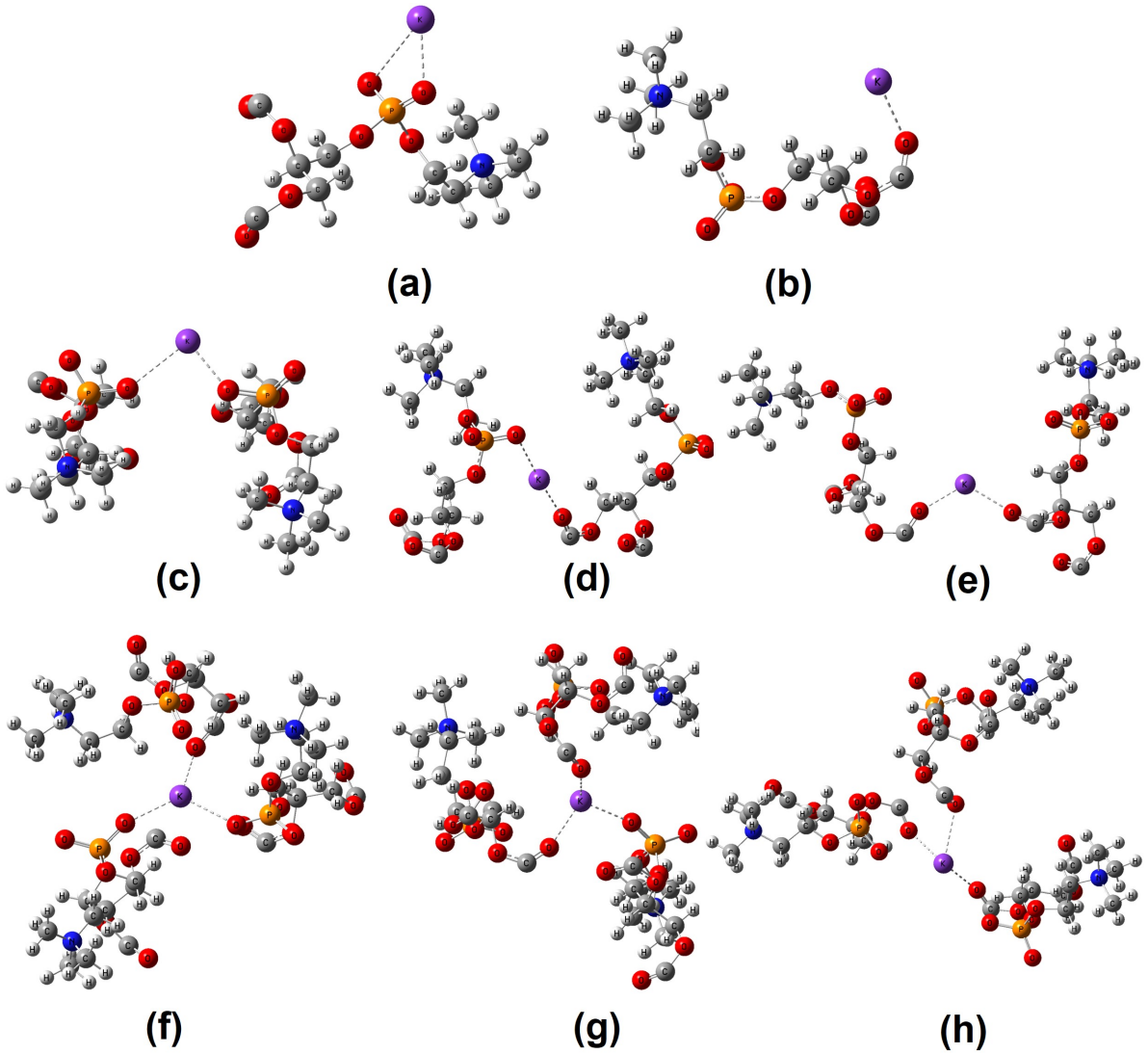

Figure S11: Extracted structures from our MD simulations for interactions of K^+ with the membrane surface with (a) 1 lipid head group through phosphatic oxygen ($O_{PO_4^-}$) (b) 1 lipid head group through carbonyl oxygen O_{CO} (c) 2 lipid head groups through 2 $O_{PO_4^-}$ (d) 2 lipid head groups through 1 $O_{PO_4^-}$ and 1 O_{CO} (e) 2 lipid head groups through 2 O_{CO} (f) 3 lipid head groups through 2 $O_{PO_4^-}$ and 1 O_{CO} (g) 3 lipid head groups through 1 $O_{PO_4^-}$ and 2 O_{CO} (h) 3 lipid head groups through 3 O_{CO}.

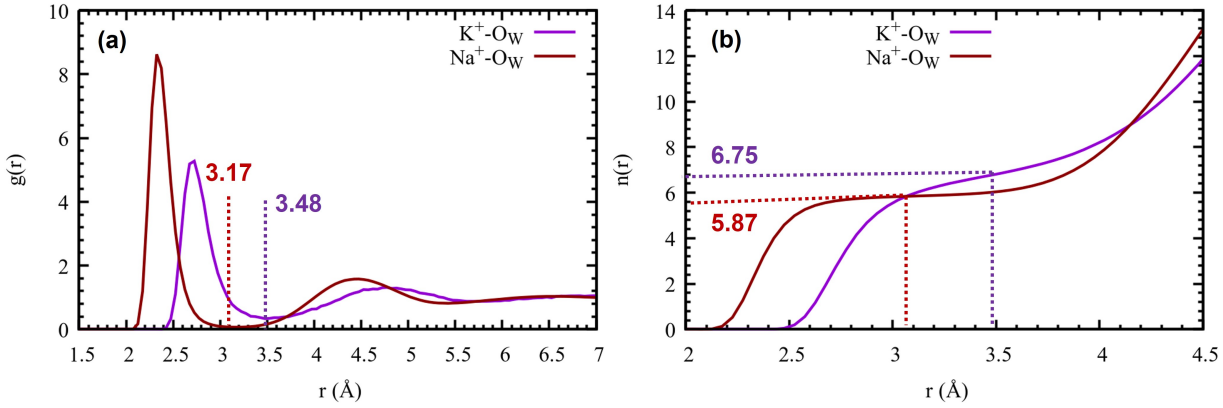

Figure S12: (a) RDFs and (b) their indefinite integrals for water oxygens (O_w) around K^+ (dark violet line) and Na^+ (dark red line) ions in salty water (400 mM KCl and 400 mM NaCl solutions, without the membrane). In (a) the vertical lines indicate the positions of the first RDF minima. (b) shows the first shell hydration numbers, which are 6.75 for K^+ and 5.87 for Na^+. The dashed lines illustrate how the number of nearest neighbors (contributing to the first hydration shell) were calculated from the first RDF minima.

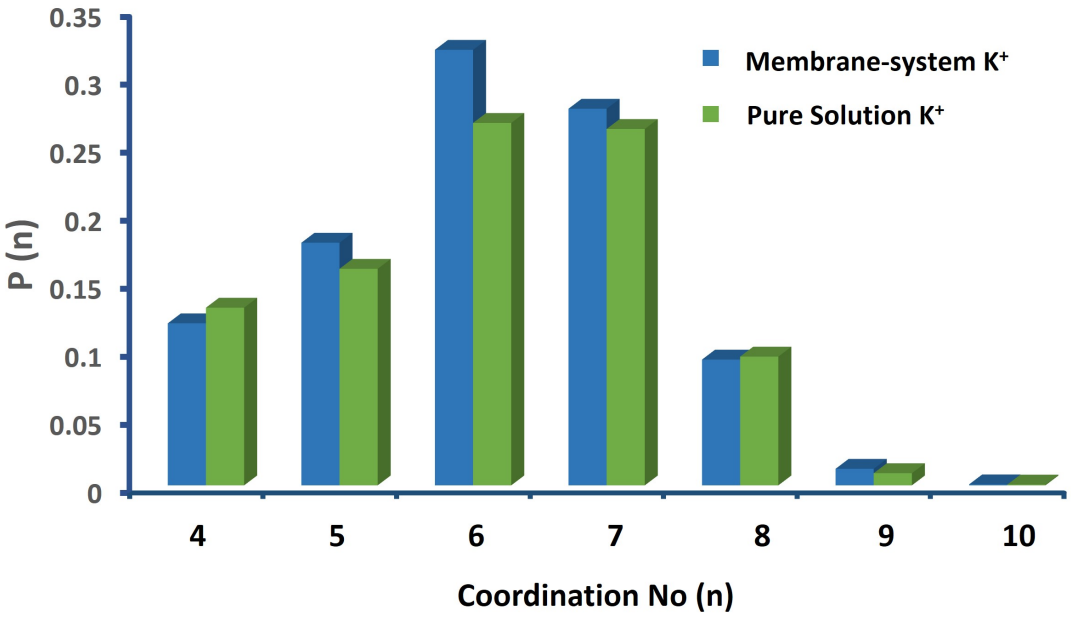

Figure S13: Comparison of hydration structure distribution between "bulk K^+" above membrane system (represented in blue color) and K^+ in pure 400 mM KCl solution (represented in green color).

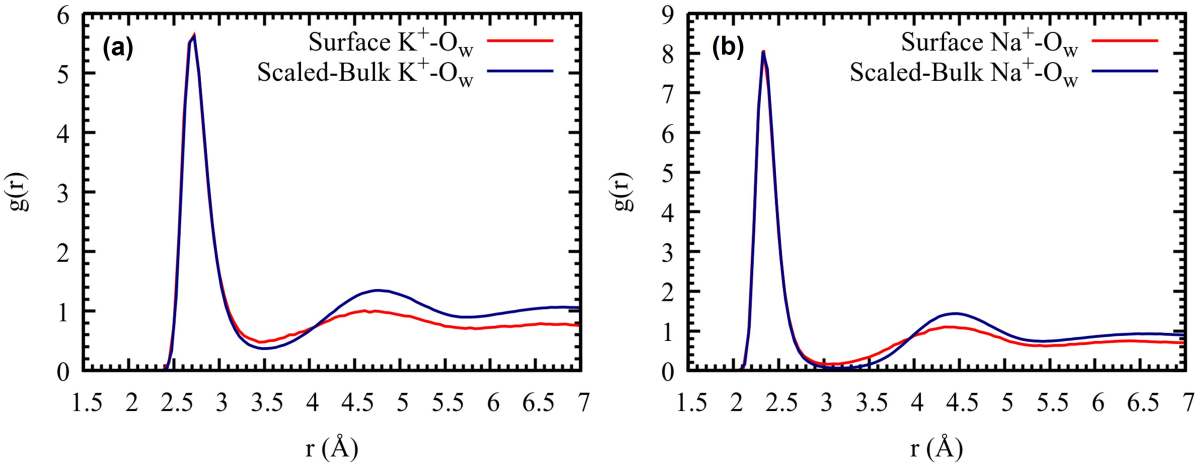

Figure S14: The *scaled* RDF for O_W atoms surrounding (a) bulk K^+ or (b) bulk Na^+ (blue line), superimposed on the RDF for water around a surface cation (red line). Scaling factors of 0.7174 and 0.6297 were applied for K^+ and Na^+, respectively. The first peak for the surface- and bulk-scaled-RDF are nearly identical, reflecting the partial absence of water ligands around a surface-cation.

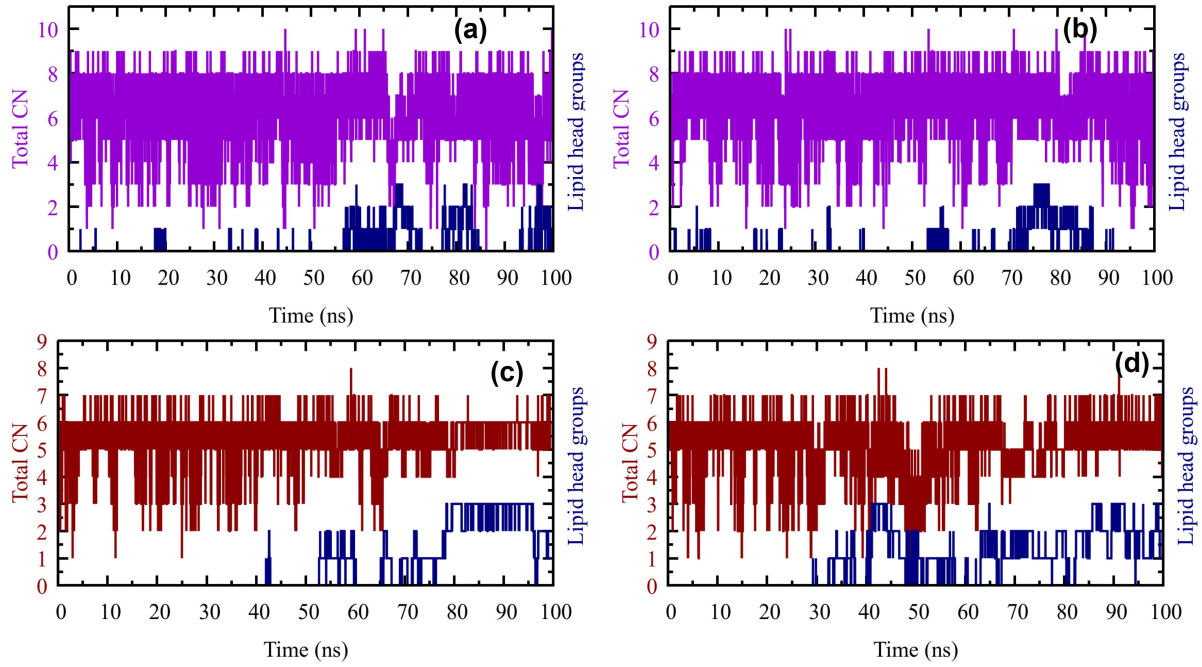

Figure S15: Time evolution of the total (water + lipid) coordination number (CN) is depicted by the upper curve and left Y-axis for (a, b) K^+ (dark-violet line), and (c, d) Na^+ (dark-red line). The number of interacting lipid head groups is shown by the lower blue curve and the right Y-axis. This shows that the total CN is almost constant, irrespective of the number of water ligands that gets replaced by lipid atoms. The indexes of the selected K^+ and Na^+ ions correspond to those in Figure 10 of the main text.

S8 Anion hydration

Figure 2 in the main text shows that K^+, and more notably Na^+, have their density peak slightly within the membrane, near the phosphate group (< 20 Å). As a result, when the cation approaches the membrane, nearly two of its water ligands are (on average) replaced by lipid atoms (Table 6). In contrast, the peak associated with the anion (Cl^-) appears around $Z = 29$ Å, as observed for various force fields[7–10] and lipids.[4] In Section 3.3 we explained this by noting that Cl^- can interact with the choline methyl groups either directly ($CH_3 \ldots Cl^-$), through a joint water molecule ($CH_3 \ldots OH_2 \ldots Cl^-$), or both. Therefore, we do not expect the Cl^- to replace more than a single water molecules in its hydration shell. To quantify this, we have compared the RDF of O_W atoms surrounding a Cl^- in the bulk and on the surface (Figure S16). From its running integral we find that as the Cl^- approaches the surface, the hydration number decreases from 6.3 to 5.9. This small drop (0.4 water molecules), considerably smaller than for the cations (nearly 2 water molecules), indicates that the anion-membrane interaction hardly affects the hydration structure of the anion.

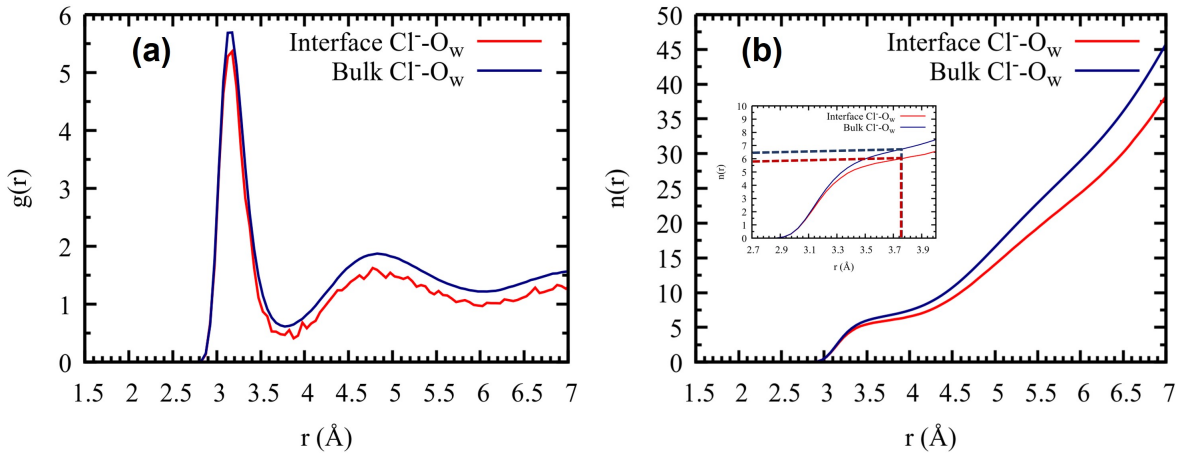

Figure S16: Radial pair distribution functions (a) and their indefinite integrals (b) for water oxygen atoms (O_w) around a Cl^- ion in the bulk (blue line) and within 2.9 Å from the membrane surface (red line) or, specifically, from the choline group (both conditions generate the same RDF). The inset represents the zoomed plot for the first hydration shell with dashed lines showing how the number of nearest neighbors is calculated.

To monitor the dynamical position of an anion, Figure S17 shows the distance from the

center of the membrane as a function of time for two representative Cl^- ions (green line), whereas others are added in Fig. S18. It is evident from Figure S17 that the anion hardly ever approaches to within 20 Å of the membrane, unlike the cations that do approach $Z < 20$, sometimes residing there for many ns. It is also seen that the few occasions when a Cl^- ion does replace two water ligands by lipid headgroup atoms occurs, almost always, when it does approach to within 20 Å from the membrane (orchid line).

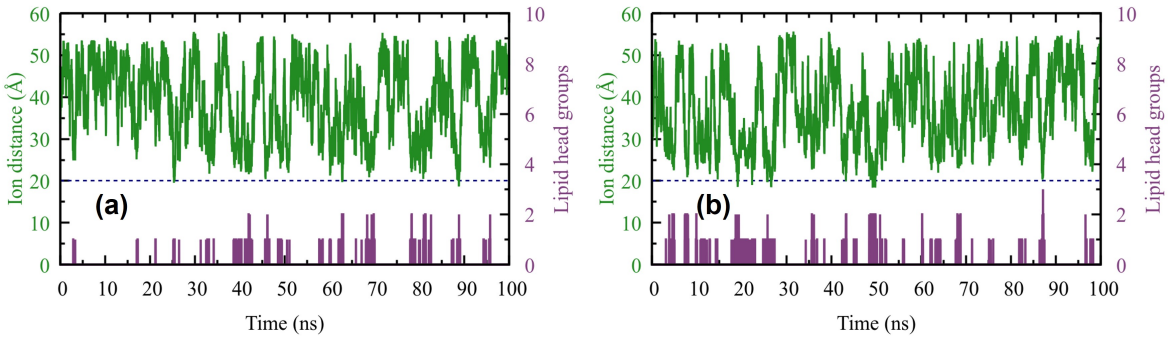

Figure S17: Distances of two representative Cl^- ions from the center of the membrane (green line and left Y-axis) along with the number of interacting lipid head groups (orchid line and right Y-axis) as a function of time during the 100 ns trajectory. The dotted line represents the average position of the membrane surface at $\sim$ 20 Å. In our distance calculations the trajectory has not been unwrapped.

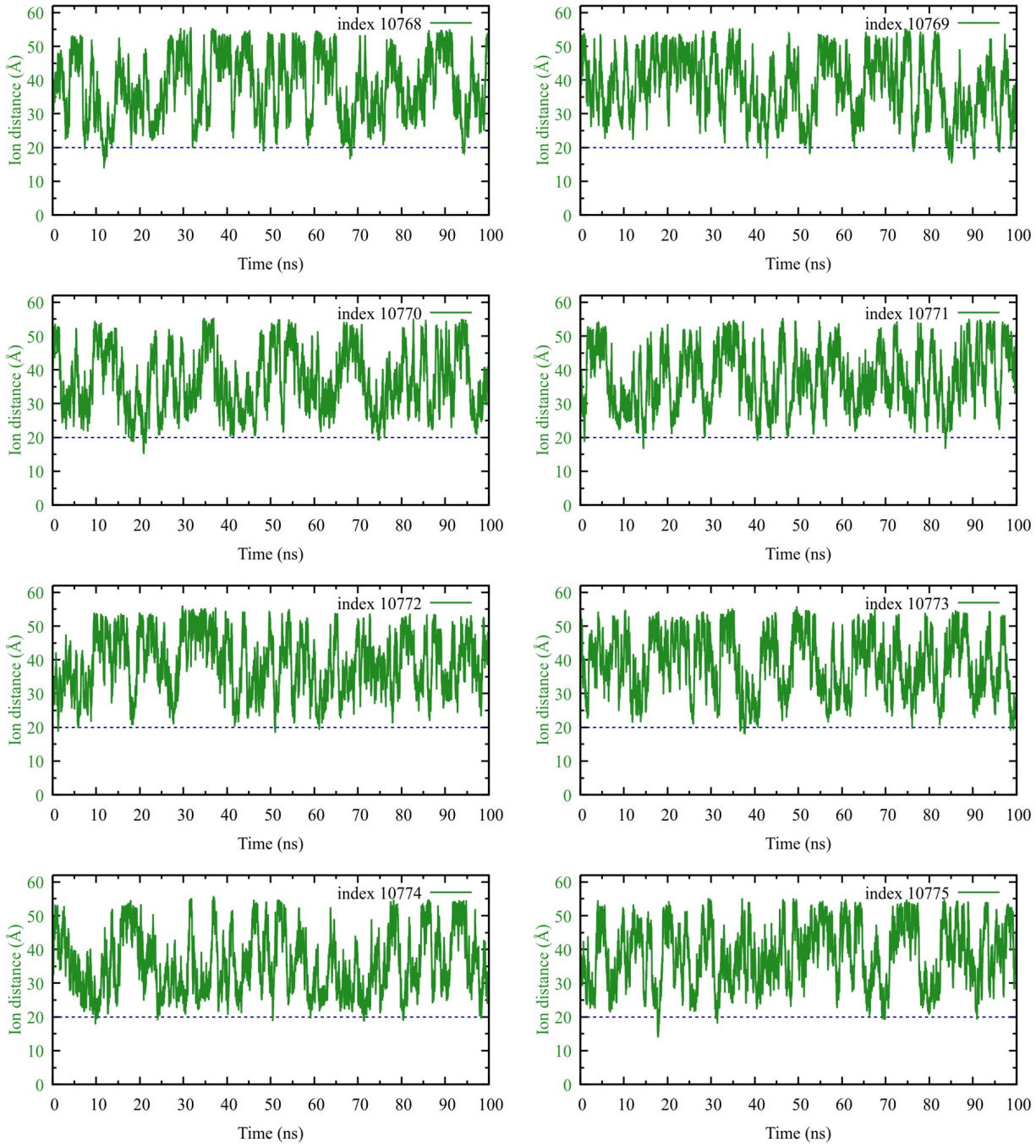

Figure S18: The distances for several Cl^- ions from the center of the membrane as a function of time during the 100 ns (wrapped, Gromacs) trajectory.

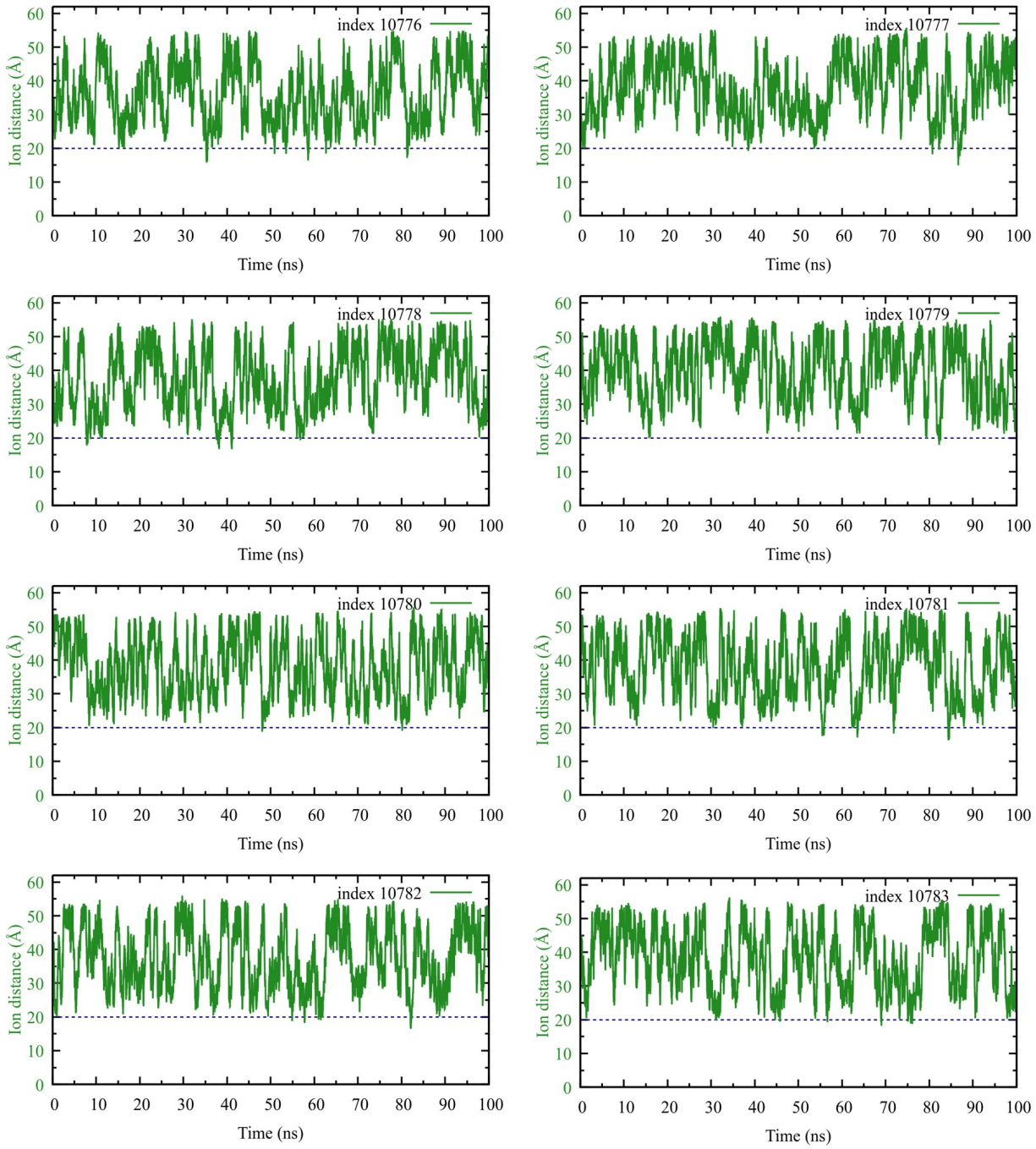

Figure S18: The distances for several Cl^- ions from the center of the membrane as a function of time during the 100 ns (wrapped, Gromacs) trajectory.

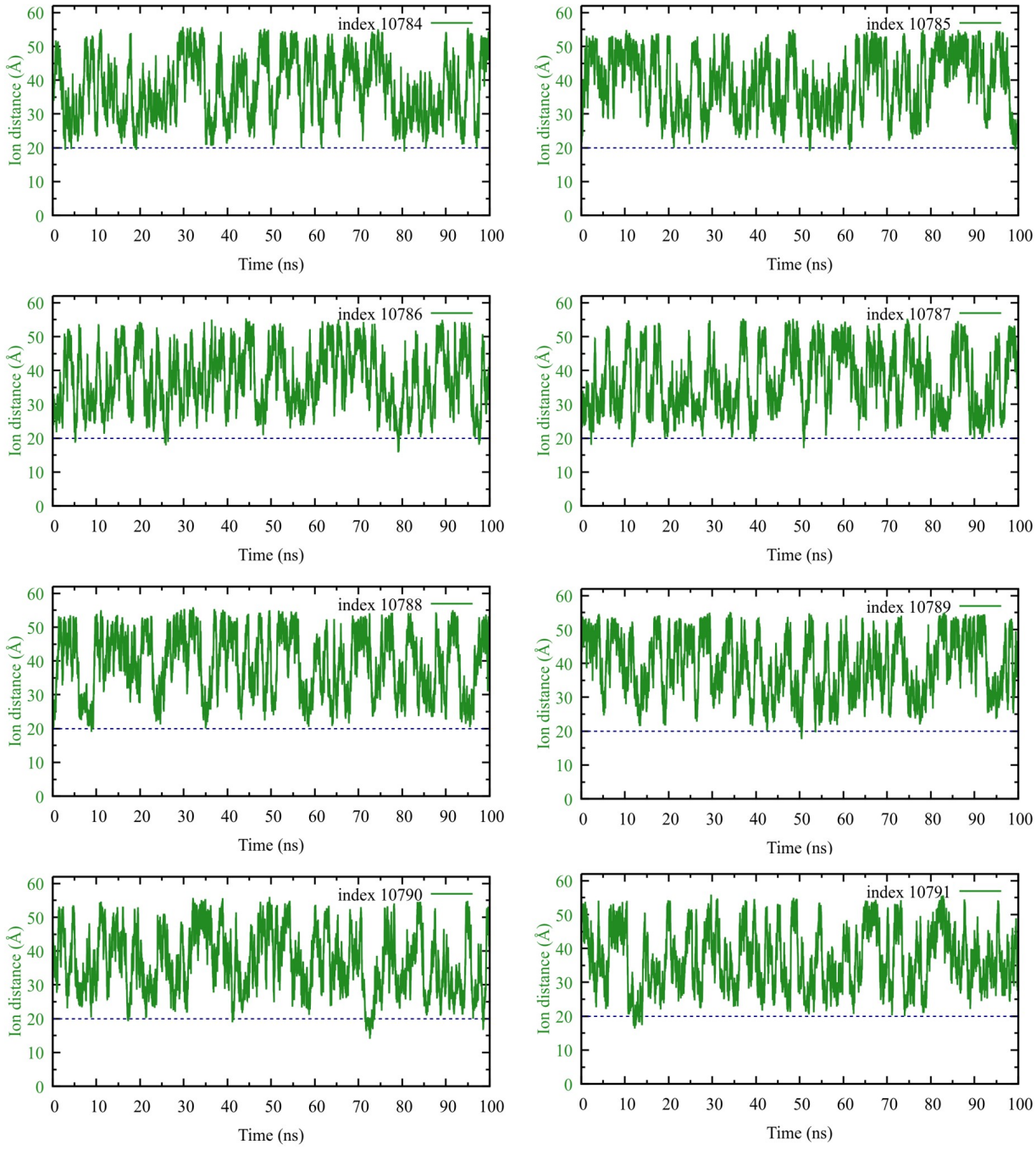

Figure S18: The distances for several Cl^- ions from the center of the membrane as a function of time during the 100 ns (wrapped, Gromacs) trajectory.

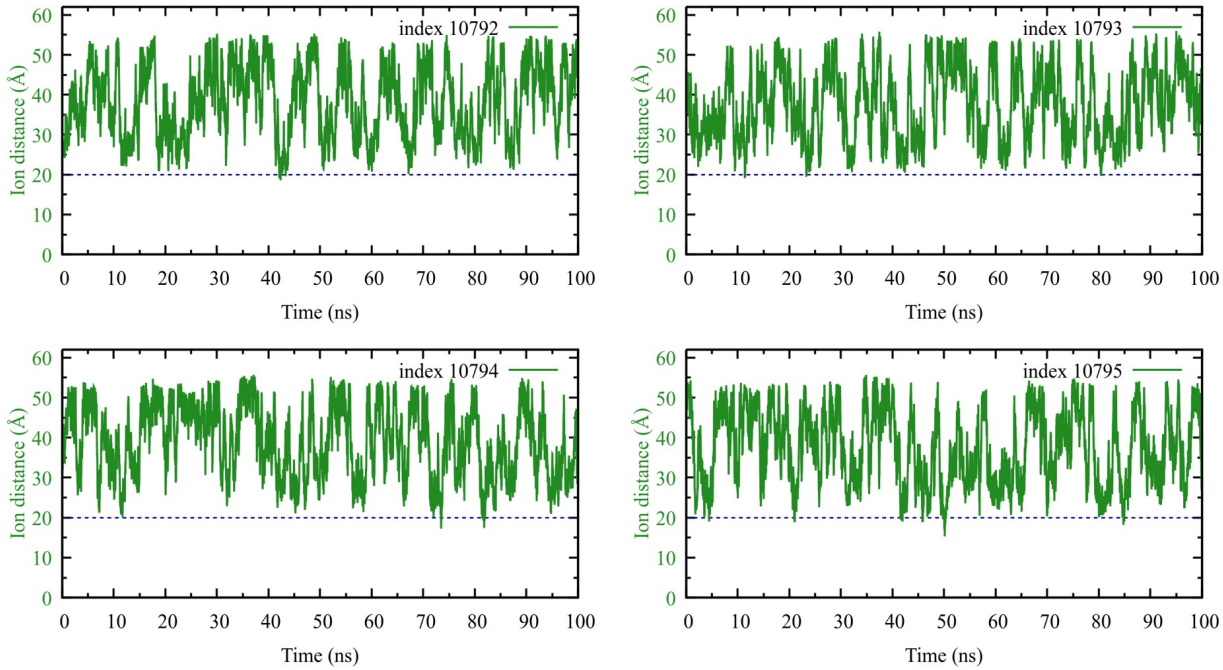

Figure S18: The distances for several Cl^- ions from the center of the membrane as a function of time during the 100 ns (wrapped, Gromacs) trajectory.

S9 Diffusion Coefficient Calculations

A particle in solution undergoes random collisions with solvent molecules from all directions. Instead of executing ballistic motion, depicted by Newton's equations, it undergoes Brownian motion following Einstein's diffusion equation

$$\frac{\partial \rho(\mathbf{r},t)}{\partial t} = \nabla[D\nabla\rho(\mathbf{r},t)] \tag{3}$$

Here $\rho(\mathbf{r},t)$ is the density of the independently diffusing particles (or, the probability density of a single diffusing particle), which depends on the particle's position vector ($\mathbf{r}$) and the time (t). D is the diffusion coefficient, which is one of the crucial dynamical properties of a particle in solution. When D is independent of $\mathbf{r}$, the diffusional motion becomes spherically symmetric, with $\nabla^2 = r^{1-d}\frac{\partial}{\partial r}r^{d-1}\frac{\partial}{\partial r}$, where r is the length of the radius vector and d the spatial dimensionality.

The solution of this spherically-symmetric partial differential equation is well-known

$$\rho(r,t) = \frac{1}{(4\pi Dt)^{d/2}}\, e^{-\frac{(r(t)-r(0))^2}{4Dt}} \tag{4}$$

where $r(t)$, and $r(0)$ represent the position of the tagged particle at time t, and its initial position, respectively. Equation 4 shows that the density of a freely diffusing particle is Gaussian in nature, with a width that increases with time. From it, one can calculate the mean square displacement (MSD) as follows:

$$\text{MSD} \equiv \langle (r(t)-r(0))^2 \rangle = 2dDt \tag{5}$$

where angular brackets, $\langle\cdot\rangle$, represent an ensemble average. From Equation 5, D can be determined from the slope of MSD vs. time, divided by $2d$. For bulk ions $2d = 6$, whereas for diffusion in a plane we divide the slope by 4.

To improve the statistics, several types of ensemble averages are utilized: averaging over identical particles (ions of a given type), over different trajectory segments (that start from different initial conditions), and using the multiple origin method. In the latter method, different trajectory segments are prepared from a single long trajectory by truncating increasingly long segments from its start.

When the solvent is very inhomogeneous (such as within a living cell) the MSD may deviate from a linear time dependence. This "abnormal" diffusion is characterized by a power-law MSD:[11]

$$\mathrm{MSD} = D_\alpha t^\alpha \tag{6}$$

where α is the anomalous diffusion exponent. When $\alpha < 1$ the process is called "subdiffusive", whereas when $\alpha > 1$ it is "superdiffusive". The coefficient D_α is a generalized diffusion coefficient. Usually, diffusion of a particle within a biological system starts off as subdiffusion, slowed down my obstacles, while switching to normal diffusion at longer times, during which the obstacles are circumvented. For cations near membrane (particularly K^+) we observe a switch to superdiffusion (Figure S24 below), perhaps switching to normal diffusion at even longer times. While we do not have evidence for this during the limited timescales of our simulations, one would not expect the diffusion rate to increase indefinitely.

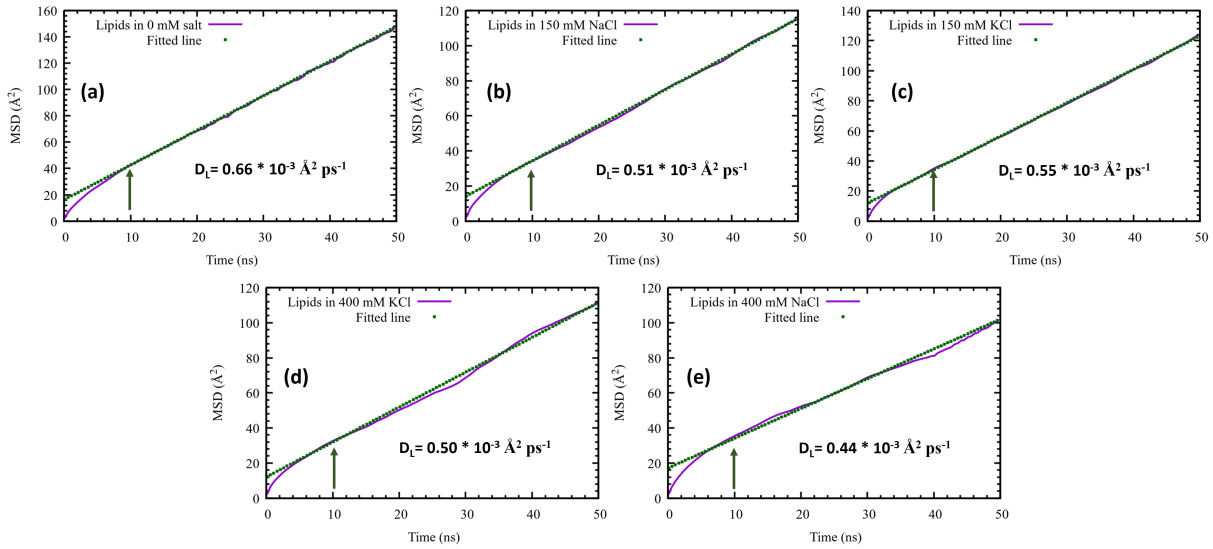

Figure S19: Mean square displacement (MSD) plots (up to 50 ns) for the phosphorus atoms of the POPC head groups solvated in (a) 0 mM salt, (b) 150 mM NaCl, (c) 150 mM KCl, (d) 400 mM KCl, and (e) 400 mM NaCl solutions, using the Lipid17 FF. Green dotted lines represent linear fits in the range 10 to 50 ns, from which D_L was extracted (Table 7a).

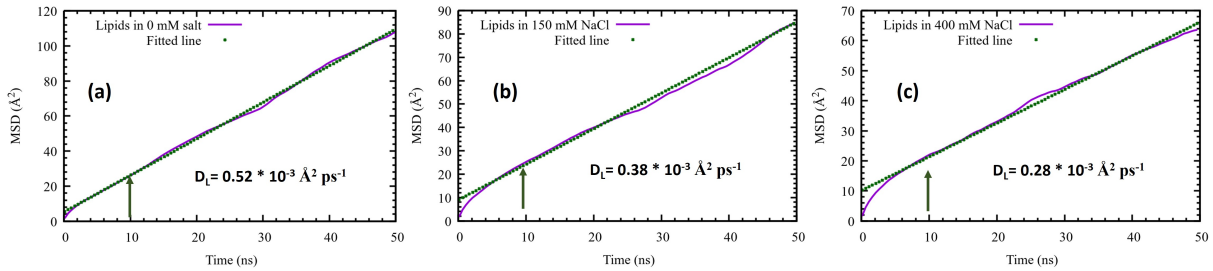

Figure S20: MSD plots (up to 50 ns) for the phosphorus atoms of the POPC head groups solvated in (a) 0 mM salt, (b) 150 mM NaCl, and (c) 400 mM NaCl solution using the Lipid21 FF. Green dotted lines represent the linear fitted lines within 10 to 50 ns, from which D_L was extracted (Table 7b).

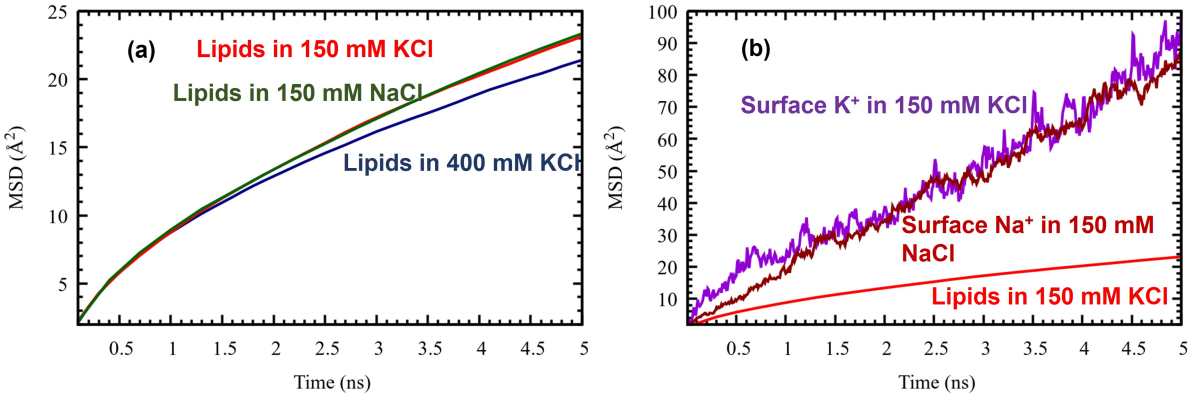

Figure S21: MSD plots for (a) the phosphorus atom of the POPC head group solvated in 150 mM KCl (red line), 150 mM NaCl (green line), and 400 mM KCl (blue line); (b) Lipid self-diffusion in 150 mM KCl (red), compared to surface K^+ in 150 mM KCl solution (violet), and surface Na^+ in 150 mM NaCl solution (brown), using the Lipid17 FF.

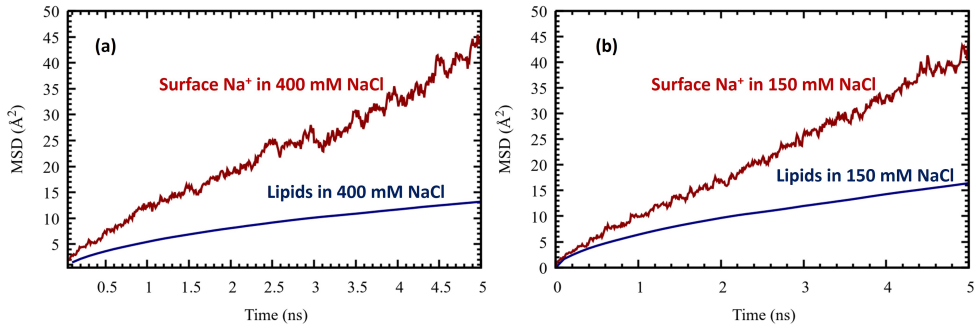

Figure S22: MSD plot illustrating lipid self-diffusion (blue) and surface Na^+ diffusion (brown) in (a) 400 mM NaCl solution, and (b) 150 mM NaCl solution using the Lipid21 force field. Evidently, the cation lateral diffusion is notably faster than lipid self-diffusion.

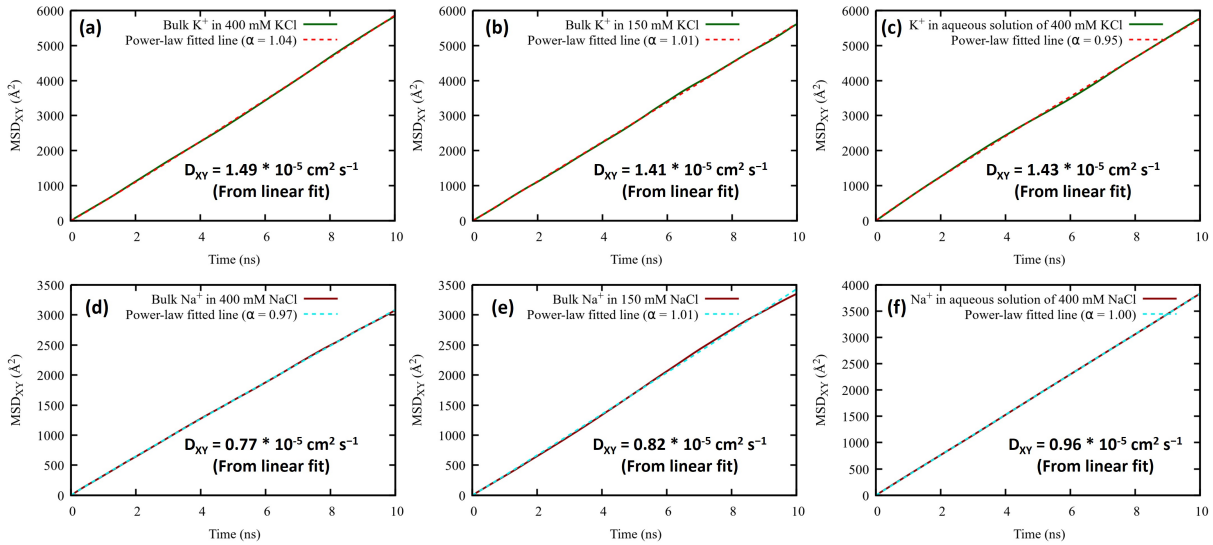

Figure S23: The MSD in the X,Y plane as a function of time (0–10 ns) for: (a) bulk K^+ in 400 mM KCl, (b) bulk K^+ in 150 mM KCl, (c) K^+ in 400 mM aqueous KCl solution, (d) bulk Na^+ in 400 mM NaCl, (e) bulk Na^+ in 150 mM NaCl, and (f) Na^+ in 400 mM aqueous NaCl solution. The dotted lines represent power-law fits. The power, α, is close to 1, indicative of normal cation diffusion in the bulk (as opposed to the abnormal lateral surface diffusion).

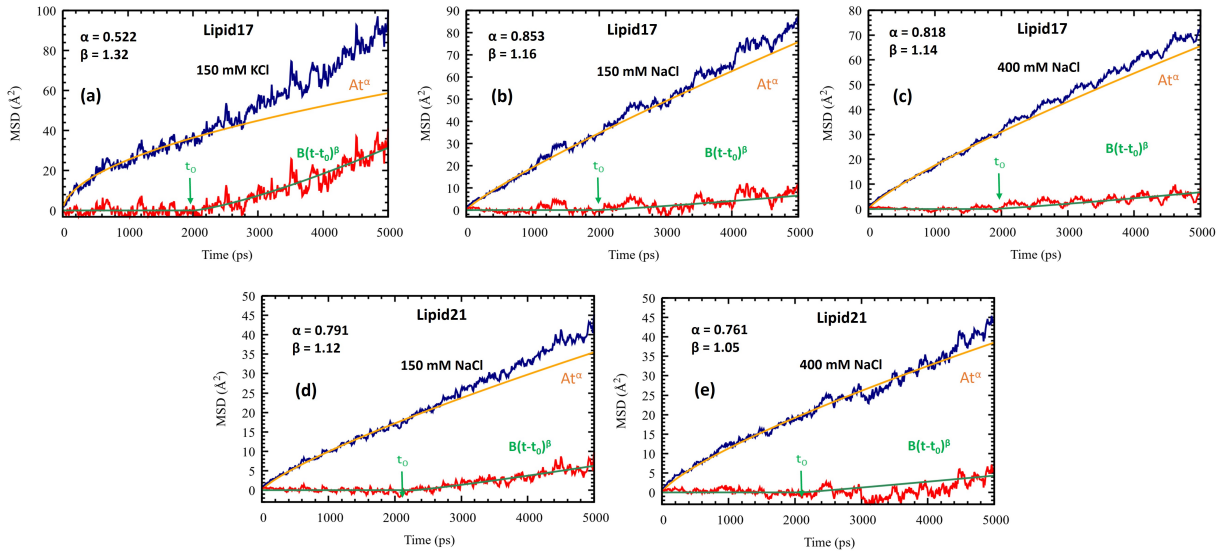

Figure S24: Fits of the tine-dependent cationic MSD (0–5 ns) to the double-Flory model, Eq. (3) in main text, for surface ions: (a) K^+ in 150 mM KCl, Lipid17 FF (b) Na^+ in 150 mM NaCl, Lipid17 FF, (c) Na^+ in 400 mM NaCl, Lipid17 FF, (d) Na^+ in 150 mM NaCl, Lipid21 FF, (e) Na^+ in 400 mM NaCl, Lipid21 FF. See also Figure 17 in main text.

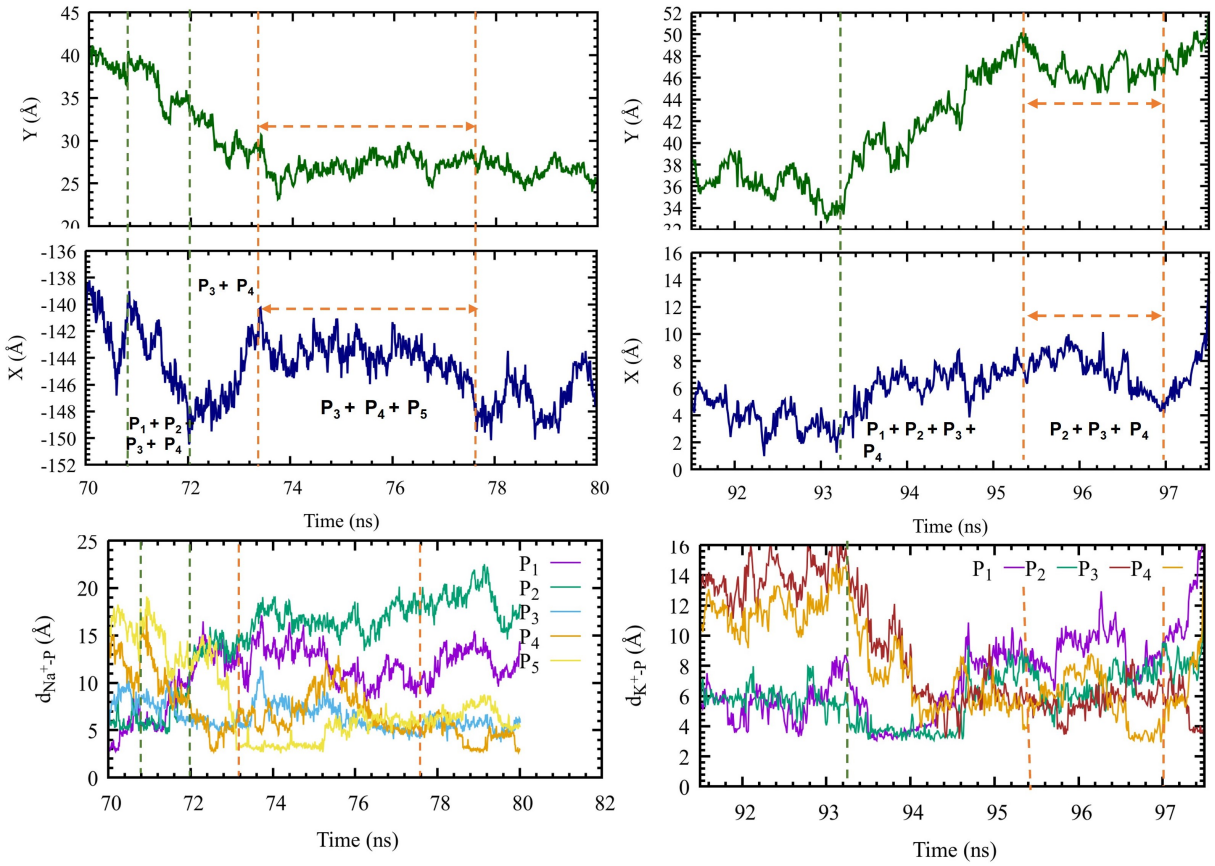

Figure S25: The top two rows illustrate the temporal evolution of the Cartesian coordinates (only X and Y) for representative Na^+ (index 10733, left column) and K^+ (index 10747, right column) ions. Lower panels display the distances between these cations and their neighbouring Pi atoms of lipid head groups within the same designated time interval.

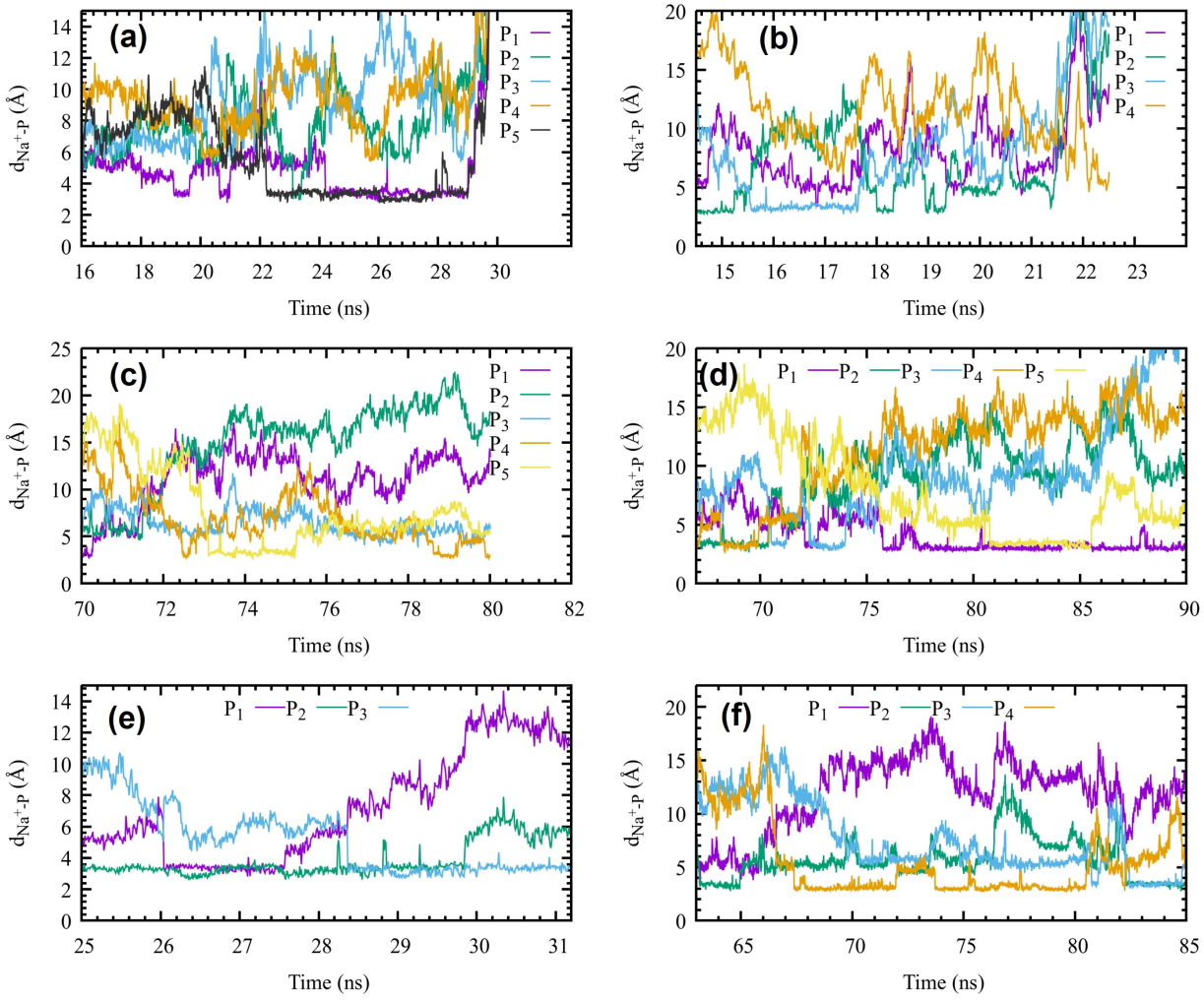

Figure S26: Temporal evolution of the distances between some representative Na^+ ions and their neighbouring P*i* atoms of lipid head groups during various time spans.

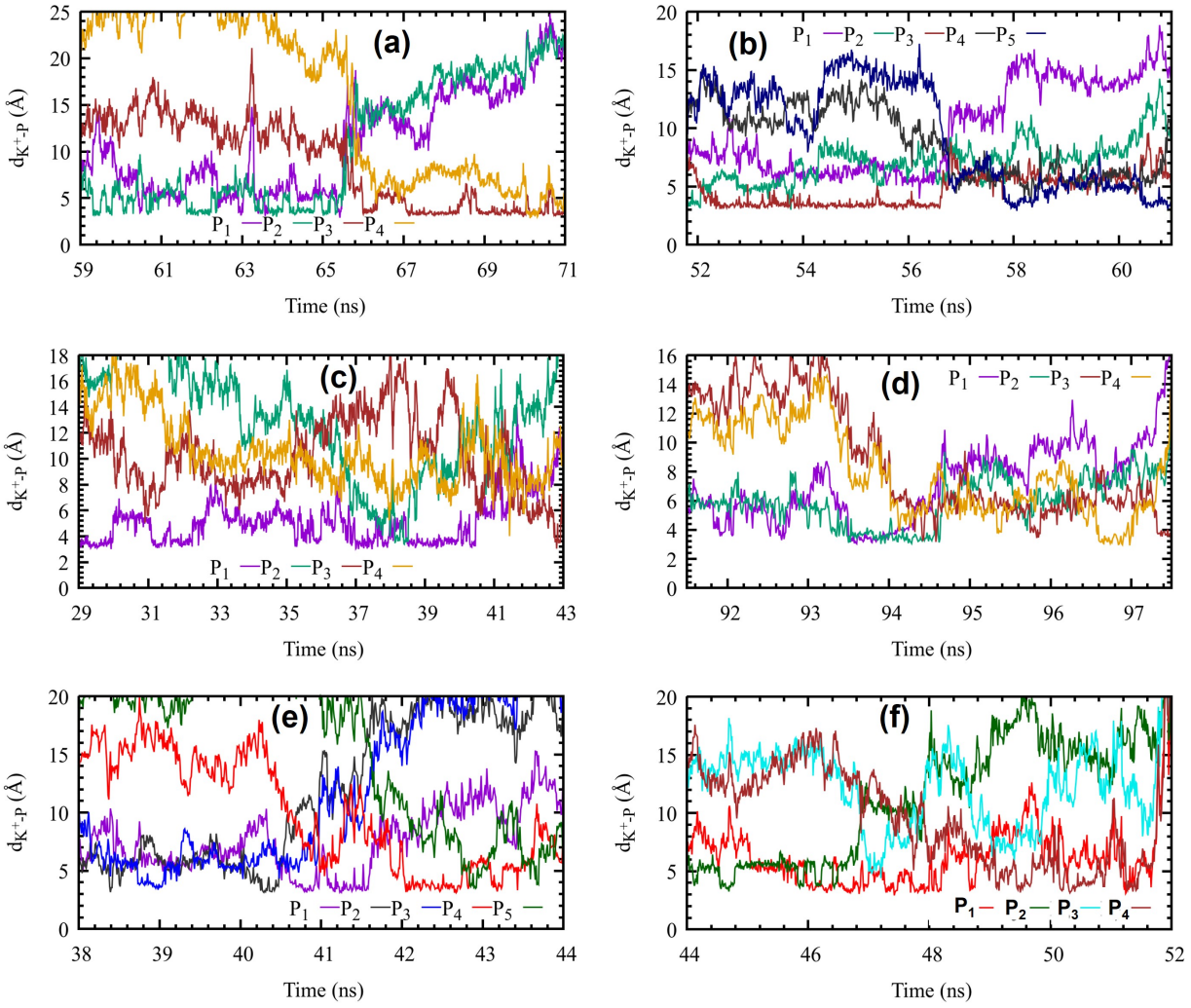

Figure S27: Temporal evolution of the distances between some representative K^+ ions and their neighbouring Pi atoms of lipid head groups during various time spans.

References

(1) Piggot, T. J.; Allison, J. R.; Sessions, R. B.; Essex, J. W. On the calculation of acyl chain order parameters from lipid simulations. *J. Chem. Theory Comput.* **2017**, *13*, 5683–5696.

(2) Ferreira, T. M.; Coreta-Gomes, F.; Ollila, O. S.; Moreno, M. J.; Vaz, W. L.; Topgaard, D. Cholesterol and POPC segmental order parameters in lipid membranes: solid state 1 H–13 C NMR and MD simulation studies. *Phys. Chem. Chem. Phys.* **2013**, *15*, 1976–1989.

(3) Essmann, U.; Perera, L.; Berkowitz, M. L.; Darden, T.; Lee, H.; Pedersen, L. G. A Smooth Particle Mesh Ewald Method. *J. Chem. Phys.* **1995**, *103*, 8577–8593.

(4) Vácha, R.; Siu, S. W.; Petrov, M.; Böckmann, R. A.; Barucha-Kraszewska, J.; Jurkiewicz, P.; Hof, M.; Berkowitz, M. L.; Jungwirth, P. Effects of Alkali Cations and Halide Anions on the DOPC Lipid Membrane. *J. Phys. Chem. A* **2009**, *113*, 7235–7243.

(5) Dourado, A. Electric Double Layer: The Good, the Bad, and the Beauty. *Electrochem* **2022**, *3*, 789–808.

(6) Oldham, K. A Gouy–Chapman–Stern Model of the Double Layer at a (Metal)/(Ionic Liquid) Interface. *J. Electroanal. Chem.* **2008**, *613*, 131–138.

(7) Böckmann, R. A.; Hac, A.; Heimburg, T.; Grubmüller, H. Effect of Sodium Chloride on a Lipid Bilayer. *Biophys. J.* **2003**, *85*, 1647–1655.

(8) Valley, C. C.; Perlmutter, J. D.; Braun, A. R.; Sachs, J. N. NaCl Interactions with Phosphatidylcholine Bilayers do not Alter Membrane Structure but Induce Long-Range Ordering of Ions and Water. *J. Membr. Biol.* **2011**, *244*, 35–42.

(9) Catte, A.; Girych, M.; Javanainen, M.; Loison, C.; Melcr, J.; Miettinen, M. S.; Monticelli, L.; Määttä, J.; Oganesyan, V. S.; Ollila, O. S. et al. Molecular Electrometer and Binding of Cations to Phospholipid Bilayers. *Phys. Chem. Chem. Phys.* **2016**, *18*, 32560–32569.

(10) Melcr, J.; Martinez-Seara, H.; Nencini, R.; Kolafa, J.; Jungwirth, P.; Ollila, O. S. Accurate Binding of Sodium and Calcium to a POPC Bilayer by Effective Inclusion of Electronic Polarization. *J. Phys. Chem. B* **2018**, *122*, 4546–4557.

(11) Metzler, R.; Klafter, J. The Restaurant at the End of the Random Walk: Recent Developments in the Description of Anomalous Transport by Fractional Dynamics. *J. Phys. A: Math. Gen.* **2004**, *37*, R161–R208.